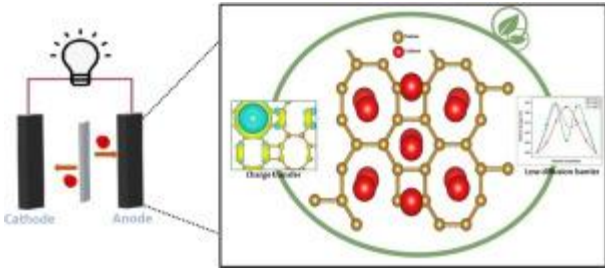
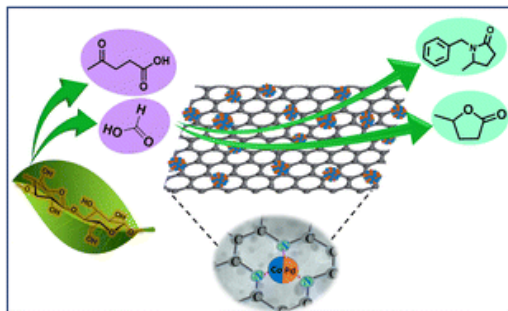


Sl. No.	<p style="text-align: center;">IIT Ropar List of Recent Publications with Abstract Coverage: April, 2023</p>
1.	<p>2-dimensional biphenylene monolayer as anode in Li ion secondary battery with high storage capacity: Acumen from density functional theory N Duhan, B Chakraborty, TJD Kumar - <i>Applied Surface Science</i>, 2023</p> <p>Abstract: Energy storage methods are cardinal for the mitigation of intermittency of renewable energy and among many technologies available, Li-ion batteries (LIBs) dominate the market on the account of their significant attributes. However, there's still room for improvement in their performance for high-end applications. Modifying the anode material can significantly affect the overall battery performance. It becomes necessary to discover a satisfactory negative electrode for more productive Li ion batteries. The present density functional theory based work examines the potential of a novel, experimentally fabricated 2D monolayer, Biphenylene having sp² carbon atoms arranged periodically in four, six, and eight-membered rings, for its application in LIBs as adequate anode. Phonon spectrum and <i>ab initio</i> molecular dynamics (AIMD) signify the dynamic and thermal stability of the nanosheet. The band structures and density of states reveal the metallic nature which is maintained after the Li (adatom) adsorption as well. The mean adsorption energies for subsequent loading of Li over the sheet vary from -0.44 to -0.15 e V. The appreciative interactions between the adatom and the monolayer are well authenticated by charge transfer analysis. The Biphenylene is observed to offer a low diffusion barrier of 0.23 eV for the Li atoms. High storage capacity of 1302 mAhg⁻¹ (almost 3.5 times higher than that of marketable Graphite), a low voltage of 0.34 V, and low volume changes (less than 3%) are noticed. This comprehensive study authenticates the capability of the 2D carbonous Biphenylene sheet as a suitable LIB negative electrode.</p> <p>Graphical abstract:</p>  <p>The graphical abstract consists of two parts. On the left, a schematic of a battery cell is shown with a lightbulb connected to the external circuit. The cell contains a cathode on the left and an anode on the right, with a separator in between. Red dots representing lithium ions are shown moving from the anode to the cathode. On the right, a circular inset shows a molecular model of a biphenylene monolayer, which is a 2D carbonous sheet with a mix of four, six, and eight-membered rings. A lithium adatom (red sphere) is shown adsorbed on the surface. A legend indicates 'Charge Transfer' and 'Lithium Adsorption Energy'.</p>
2.	<p>A CoPd nanoalloy embedded N-doped porous carbon catalyst for the selective reduction and reductive amination of levulinic acid using formic acid in water AK Kar, A Chauhan, R Srivastava - <i>Sustainable Energy & Fuels</i>, 2023</p> <p>Abstract: Biomass-derived levulinic acid and formic acid are essential platform chemicals that can fulfil the demands of renewable fuels and valuable chemicals. Using formic acid as a green and sustainable source for the reductive transformation of biomass compounds such as levulinic acid is highly exciting at the current time. Herein, formic acid-mediated levulinic acid valorization (reduction and reductive amination) was carried out in water using a CoPd nanoalloy embedded mesoporous N-doped carbon (CoPd@N-C) catalyst. CoPd@N-C was synthesized using a nanoemulsion assembly strategy, employing F127 as the soft template, followed by carbonization. The systematic modification of the textural properties and electronic properties was carefully assessed using various characterization techniques. The detailed catalyst characterization revealed the ordered porous architecture, successful formation of the CoPd nanoalloy and N-doping significantly responsible for the levulinic acid transformation to γ-</p>

valerolactone (GVL), and *N*-substituted pyrrolidone using formic acid as the reduction source. The successful CoPd nanoalloy formation and the electronically modulated surface were beneficial for efficient formic acid decomposition and levulinic acid adsorption. CoPd@N-C was robust and exhibited efficient recyclability and stability.



[A framework for crop yield estimation and change detection using image fusion of microwave and optical satellite dataset](#)

R Kaur, RK Tiwari, R Maini, S Singh - *Quaternary*, 2023

3.

Abstract: Crop yield prediction is one of the crucial components of agriculture that plays an important role in the decision-making process for sustainable agriculture. Remote sensing provides the most efficient and cost-effective solution for the measurement of important agricultural parameters such as soil moisture level, but retrieval of the soil moisture contents from coarse resolution datasets, especially microwave datasets, remains a challenging task. In the present work, a machine learning-based framework is proposed to generate the enhanced resolution soil moisture products, i.e., classified maps and change maps, using an optical-based moderate resolution imaging spectroradiometer (MODIS) and microwave-based scatterometer satellite (SCATSAT-1) datasets. In the proposed framework, nearest-neighbor-based image fusion (NNIF), artificial neural networks (ANN), and post-classification-based change detection (PCCD) have been integrated to generate thematic and change maps. To confirm the effectiveness of the proposed framework, random forest post-classification-based change detection (RFPCD) has also been implemented, and it is concluded that the proposed framework achieved better results (88.67–91.80%) as compared to the RFPCD (86.80–87.80%) in the computation of change maps with σ° -HH. This study is important in terms of crop yield prediction analysis via the delivery of enhanced-resolution soil moisture products under all weather conditions.

[A framework to describe biological entities for bioinspiration](#)

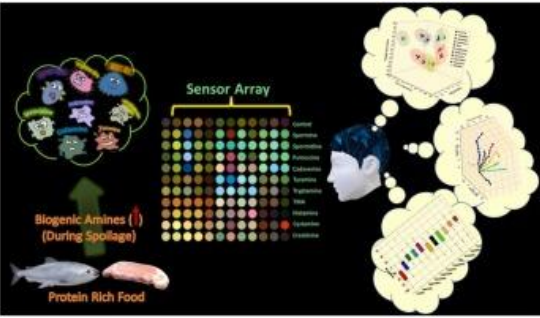
S Sharma, P Sarkar - *International Journal on Interactive Design and Manufacturing (IJIDeM)*, 2023

4.

Abstract: Designers need knowledge about biological entities for inspiration and solving problems. Most designers face difficulties in extracting knowledge about biological information. A well compiled and developed knowledge representation of biological entity can help designers and organizations to understand complex biological entity and develop concepts based on that knowledge. At present, such knowledge frameworks are unavailable. For filling this gap, a 6W framework has been developed based on the hierarchical top-down approach. This standard framework has been proposed for capturing and representing information about natural entities. This framework extracts information using formal 6W questions about function, form, behavior, structure, location and nature's intent hierarchy part wise for the natural entity. A case example (Lotus leaf) has been modeled and demonstrated using 6W framework. It has been concluded that 6W framework can capture knowledge and provide bioinspiration. A comparative SBF model has been discussed to understand the capabilities and limitations of the 6W framework.

5.	<p>A survey on seismic sensor based target detection, localization, identification, and activity recognition P Choudhary, N Goel, M Saini - ACM Computing Surveys, 2023</p> <p>Abstract: Current sensor technologies facilitate device-free and non-invasive monitoring of target activities and infrastructures to ensure a safe and inhabitable environment. Device-free techniques for sensing the surrounding environment are an emerging area of research where a target does not need to carry or attach any device to provide information about its motion or the surrounding environment. Consequently, there has been an increasing interest in device-free sensing. Seismic sensors are extremely effective tools for gathering target motion information. In this paper, we provide a comprehensive overview of the seismic sensor-based device-free sensing process and highlight the key techniques within the research field. We classify the existing literature into three categories, viz., (i) target detection, (ii) target localization, and (iii) target identification, and activity recognition. The techniques in each category are divided into multiple subcategories in a structured manner to comprehensively discuss the details. We also discuss the challenges associated with contemporary cutting-edge research and suggest potential solutions.</p>
6.	<p>A universal-input on-board charger integrated converter for srm drive targeting electric vehicle application G Kumawat, V Shah, S Payami - IEEE International Conference on Power Electronics, Drives and Energy Systems (PEDES), 2023</p> <p>Abstract: In this article, the implementation and design of a novel integrated power converter (IPC) for switched reluctance motor (SRM) drive are presented, targeting electric vehicle (EV) as an application. The proposed IPC is reconfigured as a traction converter for controlling 4-phase SRM for the drive mode of operation. For charging the battery via a residential AC outlet, i.e., AC level-1 and AC level-2 charging, the proposed IPC is employed as an integrated on-board charger (OBC) by reconfiguring it into a buck cascaded buck-boost (BuCBB) converter. The active charging inductor/s for the BuCBB configuration is/are accomplished via the windings of the 4-phase SRM. Thus, the proposed IPC fully nullifies the need of an additional off-board circuit for battery charging purposes. The integrated OBC facilitates battery charging over a universally available input voltage range, i.e., 85–265 V RMS (root mean square), with acceptable performance and efficiency. In addition, the proposed IPC configuration results in zero torque production instantaneously from the current within the phase windings during the battery charging operation. Thus, keeping the rotor stationary without employing any external braking mechanism. Experimental verification and theoretical analysis on a prototype 4-phase SRM are demonstrated to assess the efficacy of the proposed IPCs during driving and charging.</p>
7.	<p>Adversarial projections to tackle support-query shifts in few-shot meta-learning A Aimen, B Ladrecha, NC Krishnan - Machine Learning and Knowledge Discovery in Databases: Part of the Lecture Notes in Computer Science book series, 2023</p> <p>Abstract: Popular few-shot Meta-learning (ML) methods presume that a task’s support and query data are drawn from a common distribution. Recently, Bennequin et al. [4] relaxed this assumption to propose a few-shot setting where the support and query distributions differ, with disjoint yet related meta-train and meta-test support-query shifts (SQS). We relax this assumption further to a more pragmatic SQS setting (SQS+) where the meta-test SQS is anonymous and need not be related to the meta-train SQS. The state-of-the-art solution to address SQS is transductive, requiring unlabelled meta-test query data to bridge the support and query distribution gap. In contrast, we propose a theoretically grounded inductive solution - Adversarial Query Projection (AQP) for addressing SQS+ and SQS that is applicable when unlabeled meta-test query instances are unavailable. AQP can be easily integrated into the popular ML frameworks. Exhaustive empirical investigations on benchmark datasets and their</p>

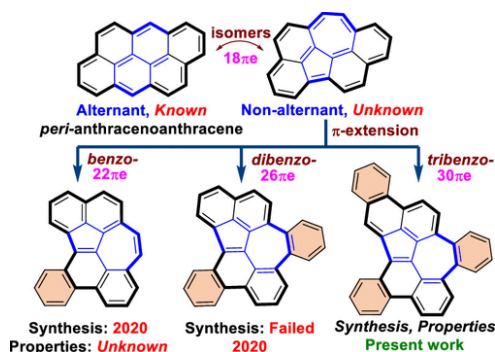
	<p>extensions, different ML approaches, and architectures establish AQP's efficacy in handling SQS+ and SQS.</p>
8.	<p>Analysis of defect associated with powder bed fusion with deep learning and explainable ai A Pratap, N Sardana, S Utomo, A John, P Karthikeyan... - 15th International Conference on Knowledge and Smart Technology (KST), 2023</p> <p>Abstract: Research into the detection, classification, and prediction of internal defects using surface morphology data of parts created via powder bed fusion-type additive manufacturing has become a hot topic in the previous decade thanks to the development of deep learning. However, there is no other evidence to evaluate the model other than accuracy and metrics. In this paper, a novel data set is compiled from various literature and other sources to evaluate the black box model using explainable artificial intelligence (XAI). The data set contains three major powder bed fusion defects: gas porosity, lack of fusion, and balling. The anomaly was initially found using convolutional neural networks (CNN) and transfer learning. Based on test data, a model comparison was performed to determine the best accuracy and an F1 score. VGG16 has outperformed all other models in terms of accuracy, with an F1 score of 98.6 percent. Further, the model has been compared with the existing state-of-the-art model for classification in the domain of powder bed fusion defects. Finally, VGG16 was employed to interpret and explain the test data set. The LIME explanations revealed that the feature predicted by the model was present in conjunction with the fault. As a result, we are confident that the proposed model with XAI would considerably improve the fairness and trustworthiness of the output result in the powder bed fusion field. This can also aid in the automation of additive manufacturing in the realm of Industry 4.0.</p>
9.	<p>Analytical modeling of three-winding tunable common-mode choke B Dwiza, S Singh, J Kalaiselvi, NB Gorla - IEEE IAS Global Conference on Renewable Energy and Hydrogen Technologies (GlobConHT), 2023</p> <p>Abstract: The common-mode (CM) noise is generally addressed using a CM choke due to its simple design and reliability. However, the performance of the CM choke degrades and the CM impedance starts decreasing after the resonant frequency. Hence, tuning the CM impedance of the CM choke is widely adapted by inserting an auxiliary winding on the CM choke core to alter the resonant frequency. Thus, in this paper, the analytical approach to estimate the CM impedance of the tunable CM choke with known external circuit parameters connected to the auxiliary winding terminals and vice-versa is presented. In addition, the estimated CM impedance profiles and the auxiliary winding parameters are simulated in MATLAB/Simulink and are validated through experimentation.</p>
10.	<p>Anticancer SAR establishment and α/β-tubulin isoform specific targeting: a detailed insight of the anticancer potential of 4H-chromene derivatives Mayank, A Singh, KU Saumya, M Joshi, N Kaur, N Garg, N Singh - New Journal of Chemistry, 2023</p> <p>Abstract: 4H-Chromene derivatives are promising anticancer compounds known to bind within the colchicine binding site of the tubulin protein. Among these, the 2-amino-4-phenyl-4H-benzo[h]chromene-3-carbonitrile-based 4H-chromenes scaffold is known to produce a significant impact on tubulin proteins. Other molecules with similar pharmacophores are also known for their colchicine binding site targeting abilities. However, tubulin is not a single protein; multiple isoforms have been reported, and some are comparatively more important under malignant conditions. Therefore, the research findings presented herein include a detailed understanding of the interaction pattern of the 2-amino-4-phenyl-4H-benzo[h]chromene-3-carbonitrile series for their colchicine binding ability against various tubulin isoforms proteins. We have established the current series anticancer potential and structural activity relationship. The series revealed promising anticancer potential, and MNC-1 was the best among all.</p>

	<p>However, a serious side effect of this scaffold is a major problem, as these derivatives indiscriminately bind to the tubulin of malignant and normal cells. However, the expression profile of tubulin isoforms was found to be different in normal and malignant cell types. Therefore, selective killing of the malignant cell seems possible by designing a 4<i>H</i>-chromenes derivative selective against particular tubulin isoforms. The insights provided herein clearly indicate the differences in the binding pattern of different 4<i>H</i>-chromenes derivatives against different tubulin isoforms. Therefore, with precise structural modification, these molecules' selective targeting against cancer cells seems quite possible.</p>
11.	<p>Azodye-based colorimetric sensor array for identification of biogenic amines: Food forensics by portable RGB-based signal readout Ranbir, G Singh, H Singh, N Kaur, N Singh - <i>Sensors and Actuators B: Chemical</i>, 2023</p> <p>Abstract: Biogenic amines (BA's) are known to be released as a result of decarboxylation of amino acids during the long storage of protein rich food products, and thus subsequently established as spoiled food markers. Consequently, the selective and sensitive detection of these biogenic amines is of utmost importance for food safety and monitoring. In this regard, herein, we demonstrate the azodye-based colorimetric sensor array for a rapid quantitative profiling of these food spoilage markers. The distinct responses towards various biogenic amines were identified and processed through automated multivariate analysis. Qualitative and quantitative determination of target analytes were performed using LDA and PSLR and results obtained showing linear correlation with different concentrations of target analytes with limit of detection values from 1.23 to 6.60 μM. For practical application, we have developed solid state cellulose paper-based sensor array which exhibits colorimetric changes for different biogenic amines; thus, makes it a potential system to conveniently monitor the concentration of analyte under investigation for food safety and monitoring through RGB analysis.</p> <p>Graphical abstract:</p>  <p style="text-align: center;">Solid State Portable Colorimetric Sensor Array for Food Forensics.</p>
12.	<p>Boron–pnictogen monolayers with a negative Poisson's ratio and excellent band edge positions for photocatalytic water splitting NVR Nulakani, TJD Kumar - <i>Physical Chemistry Chemical Physics</i>, 2023</p> <p>Abstract: Boron–pnictogen (BX; X = N, P, As, Sb) materials, in most cases, share structural characteristics with the aesthetically pleasing architectures of carbon allotropes. Recently, a two-dimensional (2D) metallic carbon allotrope (biphenylene) has been synthesized using experimental methods. In the present study, we have examined the structural stabilities, mechanical properties, and electronic fingerprints of biphenylene analogs of boron–pnictogen (bp-BX) monolayers using state-of-the-art electronic structure theory. We have validated the dynamical stability using phonon band dispersion analysis and thermal stabilities using <i>ab initio</i> molecular dynamics studies. The bp-BX monolayers exhibit a positive (bp-BN) and</p>

	<p>negative (bp-BP, bp-BAs, bp-BSb) Poisson's ratio with anisotropic mechanical properties in the 2D plane. Electronic structure studies unveil that the bp-BX monolayers show semiconducting properties with an energy gap of 4.50, 1.30, 2.28 and 1.24 eV for X = N, P, As and Sb, respectively. Computed band edge positions, lighter charge carriers and optimally separated hole and electron regions indicate that the bp-BX monolayers can serve as potential candidates for the metal-free water dissociation reaction using photocatalysis.</p>
13.	<p>Burning and w-burning of geometric graphs B Gorain, AT Gupta, SA Lokhande, K Mondal, S Pandit - <i>Discrete Applied Mathematics</i>, 2023</p> <p>Abstract: Graph burning runs on discrete time-steps. The aim is to burn all the vertices in a given graph using a minimum number of time-steps. This number is known to be the burning number of the graph. The spread of social influence, an alarm, or a social contagion can be modeled using graph burning. The less the burning number, the faster the spread. It is well-known that the optimal burning of general graphs is NP-complete. Further, graph burning has been shown to be NP-complete on a vast majority classes of graphs. Approximation results also exist for several graph classes. In this article, we show that the burning problem is NP-complete on connected interval graphs and permutation graphs. We also study the burning properties of grids. More precisely, we show that the lower bound of the burning number of a grid ($l \times b$) is at least $(l \times b)^{1/3}$. We provide a 2-approximation for burning a square grid. We extend the study of the w-burning problem, a variation of the graph burning problem where we allow a constant w number of vertices to be burnt in any time-step. We prove that w-burning of interval, spider, and permutation graphs are NP-complete for any constant w. We also provide a 2-approximation for the w-burning problem on trees</p>
14.	<p>Comparative analysis of tool wear in micro-milling of wrought and selective laser melted Ti6Al4V J Airao, H Kishore, CK Nirala – <i>Wear</i>, 2023</p> <p>Abstract: The parts produced by additive manufacturing (AM) are not usually appropriate for direct applications and require several post-processing operations. Micro-milling, as a most common post-processing operation in micromachining, is performed considering selective laser melted (SLM) Ti6Al4V as the workpiece under dry condition. The experiments are conducted considering a constant cutting speed and axial depth using a TiAlSiN-coated tungsten carbide end mill of $\text{Ø}300 \mu\text{m}$. It employs two different feed rates considering the size effect imposed by the edge radius of the micro end mill. The micro-milling performances for the SLM Ti6Al4V are compared with the performance for wrought Ti6Al4V. The outcomes, such as tool wear and surface characteristics, are examined for both the materials. Equiaxed grains, exhibiting higher ductile nature of wrought Ti6Al4V, produces adhesive tool wear, BUE formation and poor surface topography at both feed rates. Alternatively, the lamella microstructure of SLM Ti6Al4V, exhibiting relatively high hardness, produces less adhesive tool wear and BUE formation; instead, it generates more abrasion of the tool and hence increases the surface roughness. Quantitatively, the cutting-edge radius enlarges by 18–37% and 10–34% for wrought and SLM Ti6Al4V, respectively. Moreover, the SLM Ti6Al4V shows an 8–10.6% lower average surface roughness value than wrought Ti6Al4V.</p>
15.	<p>Comparative study of modelling flows in porous media for engineering applications using finite volume and artificial neural network methods P Makauskas, M Pal, V Kulkarni, AS Kashyap, H Tyagi - <i>Engineering with Computers</i>, 2023</p> <p>Abstract: A neural solution methodology, using a feed-forward and a convolutional neural networks, is presented for general tensor elliptic pressure equation with discontinuous coefficients. The methodology is applicable for solving single-phase flow in porous medium, which is traditionally solved using numerical schemes like finite-volume methods. The neural solution to elliptic pressure equation is based on machine learning algorithms and could serve as</p>

	<p>a more effective alternative to finite volume schemes like two-point or multi-point discretization schemes (TPFA or MPFA) for faster and more accurate solution of elliptic pressure equation. Series of 1D and 2D test cases, where the results of Neural solutions are compared to numerical solutions obtained using two-point schemes with range of heterogeneities, are also presented to demonstrate general applicability and accuracy of the Neural solution method.</p>
16.	<p>Computationally efficient optimal design of hygrothermally stable laminate with bend–twist coupling by analytical and numerical strategy NK Shakya, SS Padhee - <i>Composites Part A: Applied Science and Manufacturing</i>, 2023</p> <p>Abstract: Bent–twist coupling can be achieved by both asymmetric and symmetric laminate composites. Asymmetric laminates exhibit both in-plane and out-of-plane hygrothermal deformations, while symmetric laminates exhibit only in-plane hygrothermal deformation. These hygrothermal deformations lead to dimensional instability of structures in operational conditions due to temperature and moisture changes and hence need to be eliminated. Two generalized stacking sequences have been proposed, which inherently satisfy the hygrothermal stability conditions and provide the required bend–twist coupling. Optimization has been done by both analytical and numerical techniques. These optimized results are verified by comparing them with conventional constrained numerical optimization results, showing the excellent agreement between them. The comparison of computational time data suggests that the proposed stacking sequence is more computationally efficient than constrained numerical optimization. The sensitivity analysis has been performed to examine the robustness of the optimized sequence, suggesting that the error distribution is within $\pm 6\%$.</p>
17.	<p>Conductive polythiophene/graphitic-carbon nitride nanocomposite for the detection of ethanol mixing in petrol A Husain, S Ahmad, SA Alqarni, SJ Almeahdi... - <i>RSC Advances</i>, 2023</p> <p>Abstract: The automobile vehicles must be operated on fuel containing no more than 10% ethanol. Use of fuel having more than 10% ethanol may cause engine malfunction, starting and running issues, and material degradation. These negative impacts could cause irreversible damage to the vehicles. Therefore, ethanol mixing in petrol should be controlled below 10% level. The current work is the first to report sensing of ethanol mixing in petrol with reference to the variation in the DC electrical conductivity of polythiophene/graphitic-carbon nitride (PTh/gC₃N₄) nanocomposite. The <i>in situ</i> chemical oxidative method of polymerization was used for synthesizing PTh and PTh/gC₃N₄ nanocomposite. Fourier transform infrared spectroscopy (FT-IR), X-rays diffraction (XRD), thermo-gravimetric analysis (TGA), transmittance electron microscopy (TEM) as well as scanning electron microscopy (SEM) analysis were used for confirmation of the structure along with morphology of the PTh and PTh/gC₃N₄ nanocomposite. The thermal stability of DC electrical conductivity of PTh and PTh/gC₃N₄ nanocomposite were tested under isothermal and cyclic ageing condition. The sensing response of PTh and PTh/gC₃N₄ nanocomposite as a function of DC electrical conductivity were recorded in petrol and ethanol atmosphere. The sensing response of PTh/g-C₃N₄ nanocomposite in petrol atmosphere was 6.1 times higher than that of PTh with lower detection limit to 0.005 v/v% of ethanol prepared in <i>n</i>-hexane.</p>
18.	<p>Constructing 1-ethoxyphenanthro[9,10-<i>e</i>]acephenanthrylene for the synthesis of a polyaromatic hydrocarbon containing a formal azulene unit PK Sharma, A Babbar, D Mallick, S Das - <i>The Journal of Organic Chemistry</i>, 2023</p> <p>Abstract: <i>peri</i>-Acenoacenes are attractive synthetic targets, but their non-benzenoid isomeric counterparts were unnoticed. 1-Ethoxyphenanthro[9,10-<i>e</i>]acephenanthrylene 8 was synthesized and converted to azulene-embedded 9, which is a tribenzo-fused non-alternant isomeric motif of <i>peri</i>-anthracenoanthracene. Aromaticity and single-crystal analyses suggested a formal azulene core for 9, which showed a smaller highest occupied molecular orbital (HOMO)–lowest</p>

unoccupied molecular orbital (LUMO) energy gap with a charge-transfer absorption band and brighter fluorescence than **8** (quantum yield (Φ): **9** = 41.8%, **8** = 8.9%). The reduction potentials of **8** and **9** were nearly identical, and the observations were further supported by density functional theory (DFT) calculations.



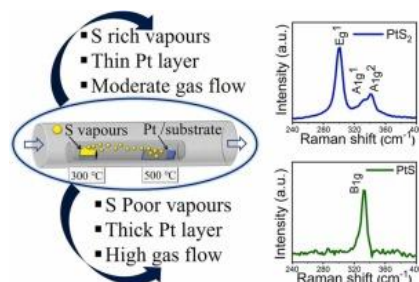
[Controlled and tunable growth of ambient stable 2D PtS₂ thin film and its high-performance broadband photodetectors](#)

G Bassi, R Wadhwa, S Deswal, P Kumar, M Kumar - *Journal of Alloys and Compounds*, 2023

19.

Abstract: PtS₂, a group-10 transition metal dichalcogenide (TMDC), has recently attracted enormous interest owing to its tunable band gap (0.25–1.6 eV), high carrier mobility, and large current on-off ratio of the devices. In contrast to other TMDCs, the growth of PtS₂ is more difficult, partly due to the nobility of Pt and partly due to the easier formation of the more stable PtS phase rather than PtS₂. Herein, we investigate the effect of critical growth parameters like sulfur amount, Pt thickness and gas flow rate for the control and large area growth of PtS₂ via thermal assisted conversion process in atmospheric chemical vapour deposition. The detailed characterization using Raman and X-ray photoelectron spectroscopy (XPS) suggests a controlled transition from PtS to PtS₂, which can be obtained by fine tuning of these growth parameters. Furthermore, the optimized growth condition of PtS₂ is highly reproducible and can be grown on varieties of substrates like SiO₂/Si, sapphire, p-type Si, and even on flexible mica substrate. Finally, a high-performance PtS₂ photodetector (PD) was fabricated on different substrates. The PD fabricated on SiO₂/Si substrate with a detection range covering from visible to NIR region (400–1100 nm) showed a high responsivity and detectivity of 31.38 AW⁻¹ and 3.92 × 10¹³ Jones, respectively, under 900 nm illumination at a low bias of 1 V. This work demonstrates an effective approach to control the growth of PtS₂ on varieties of substrate for high-performance next-generation photodetector for NIR photodetection applications.

Graphical abstract:



20.

[CoSMoR: Decoding decision-making process along continuous composition pathways in machine learning models trained for material properties](#)

D Beniwal, PK Ray - *Physical Review Materials*, 2023

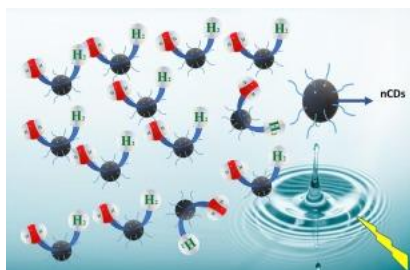
	<p>Abstract: A key challenge in materials informatics is to decode the decision-making process of machine learning (ML) models that have been trained to predict material properties. The existing methods usually rank alloy features based on importance metrics and do not provide material-specific fundamental insights. Here, we present the Compositional Stimulus and Model Response (CoSMoR) framework that can be applied to any composition-based ML model (irrespective of the algorithm used) to calculate the exact contribution of each feature towards the manifestation of target material property along a continuous compositional pathway. CoSMoR utilizes the local partial dependencies of target property with respect to each feature and combines it with feature variations associated with discretized compositional variations to measure exact feature contributions. We showcase the importance of CoSMoR through implementation on phase-selection problem in multiprincipal element alloys (MPEAs), wherein it leads to physical insights into phase transitions. A detailed overview of the framework, along with the codes and step-by-step implementation of the algorithm, has been provided to enable extension to new or preexistent models.</p>
21.	<p>Design and testing of pressure ulcers preventive bed for neonates in neonatal intensive care units AN Mallick, M Kumar, B Basumatary, K Arora, AK Sahani - IEEE Transactions on Medical Robotics and Bionics, 2023</p> <p>Abstract: In neonatal intensive care units (NICUs), preterm infants lie down immobile for long hours in a particular position, which makes them susceptible to develop pressure ulcers (PUs). These are developed due to continuous constant contact pressure generated by the self-weight of the infants with bed surfaces on their sensitive skin, which is 60% less than the thickness of an adult and hampers blood flow from the subcutaneous areas. Therefore, it is necessary to change the posture in a periodic manner. Hospitals manage the position changes by nursing staff, which is of limited effect and puts additional loads on them. Hence, in this paper, an anti-pressure ulcer bed was designed and tested to prevent pressure ulcers and also help in reducing the effort of nurses. The contact pressure of both the neonatal phantom and neonatal baby with the silicone-made bed surface was automatically varied by fluid pressure in the multi-channels based on the actuation mechanism (which rises alternately in inflated regions and falls in deflated regions), and it was measured using the force sensors. The demonstrated work was carried out in finite element modeling (FEM) using Abaqus to validate the results. We anticipate that itll reduce the risk of pressure ulcers, confirming the designed beds performance.</p>
22.	<p>Design flood estimation based on synthetic unit hydrograph method for an indian catchment R Lall, S Chavan – Copernicus Meetings: A conference proceeding, 2023</p> <p>Abstract: Design flood estimation is necessary for the effective planning and management of various hydrologic structures such as dams. Mostly these structures are located in remote locations where observed streamflow data is seldom available. There is a need to develop effective strategies to predict reliable estimates of design flood at ungauged locations. The concept of Synthetic Unit Hydrograph (e.g., Snyder’s method, Soil Conservation Service method, Taylor and Schwarz method, Mitchell’s method, etc.) that considers the use of catchment descriptors related to stream network and topography in predicting the design flood estimates at ungauged locations is being widely used. The Central Water Commission (CWC) method was specifically developed for predicting reliable estimates of design floods at the ungauged locations in India. In the present study, we have estimated the design flood estimate for Swan river which is a tributary of Satluj River in India located in upper Indo-Ganga plains. Design flood estimates are obtained corresponding to a rainfall input having return periods of 100 years. In addition, physical upper bound of precipitation i.e. probable maximum precipitation is also considered for estimating the probable maximum flood (PMF) for the catchment. The design flood corresponding to 100-year return period rainfall is found to be 2537 cumecs while the PMF is observed to be about 7863 cumecs. Further, a comparative study between the CWC method-based design flood estimate and design flood estimates based on</p>

	<p>Snyder's method, Soil Conservation Service method, Taylor and Schwarz method, and Mitchell's method are performed. These estimates of design flood can be used to plan river training works on Swan river.</p>
23.	<p>Determination of joint roughness coefficient using a cost-effective photogrammetry technique S Rohilla, R Sebastian - Bulletin of Engineering Geology and the Environment, 2023</p> <p>Abstract: The presence of discontinuities in the rock mass is extremely crucial in many engineering applications of rock mechanics. The estimation of the joint roughness coefficient (JRC) utilising easily accessible camera-friendly devices and application software has recently gained prominence. The joint roughness coefficient of a jointed rough surface may be calculated using either contact methods (physically contacting the surface to get the profile) or non-contact methods (extraction of the profile without physically touching the surface using laser profilometry or 3D laser scanning and photogrammetry techniques). The 3D laser scanner is widely used for its accuracy in obtaining the surface topography of rock masses; however, the practice is often uneconomical due to the high equipment cost. In this study, the smartphone photogrammetry technology is used to extract the three-dimensional surface topography of a jointed rough surface in order to evaluate the JRC. For the comparative study, the surface profile was retrieved using a surface profilometer, 3D scanner and photogrammetry method. The JRC values for the surface profiles gathered through smartphone photogrammetry, 3D scanning and surface profilometer have been estimated using visual analysis, fractal dimension and statistical techniques. The study found that the surface profile generated using the photogrammetric approach utilising smartphone delivers more realistic profiling than the surface profilometer because of the lower least count and greater precision. The predicted JRC values for smartphone photogrammetry profiles agreed well with the JRC values obtained for 3D scanner and surface profilometer profiles.</p>
24.	<p>Dynamic data advertising and packet loss analysis using ble legacy advertising S Gautam, R Verma, S Kumar - IEEE Transactions on Mobile Computing, 2023</p> <p>Abstract: Bluetooth Low energy (BLE) advertisements have great potential in Internet of Things applications like monitoring systems, which involve the real-time transfer of data collected from sensors interfaced to multiple power-constrained devices. Since sensor data conveys information about the present state of the system, packet loss is vital in such applications. The paper proposes a customized BLE legacy advertising packet structure to advertise dynamic sensor data, and proposes two techniques: One-Set-Multiple-Events (OSME) and One-Set-X-Events (OSXE), to advertise the dynamic sensor data using the non-connectable and non-scannable undirected advertising mode of BLE. Using appropriate advertising parameters with OSXE, each advertising packet gets successfully advertised X times, whereas OSME neither guarantees successful advertisement of all the packets, nor does it allow control over the number of transmitted copies of each packet. Using OSXE, experimental analysis is carried out to study packet loss when single BLE node transmits alone, and when 25 nodes transmit simultaneously. Mathematical analysis has been carried out for packet collision for multiple nodes. Experimental results show that packet loss is also impacted by factors like advertising set duration, scan window, scanner's link layer activities like advertising report generation and channel switching. Using OSXE, packet loss close to 0% is obtained for X=3 when 25 nodes advertise simultaneously.</p>
25.	<p>Effect of conductivity coefficients on dc breakdown strength of multilayer cable P Muppala, CC Reddy - IEEE 6th International Conference on Condition Assessment Techniques in Electrical Systems (CATCON), 2023</p> <p>Abstract: In a DC cable joint, the material properties and size of rubber layer vary with jointing kit manufacturers. Hence the conductivity coefficients of rubber are more likely to vary when compared to that of XLPE. The sensitivity of breakdown strength of cable insulation to stress</p>

	<p>and temperature coefficients is already established in literature. Hence, in this paper, the authors have performed a preliminary analysis on the effect of rubber conductivity coefficients on the breakdown strength of concentric XLPE-Rubber cable. The effect of rubber thickness in proportion to XLPE thickness on the breakdown strength of multilayer cable was also investigated at different stress coefficient ranges. The results are believed to be useful for jointing kit manufacturers.</p>
26.	<p>Effect of doping IVB, VB and VIB elements on structure, stability, elastic and electronic properties of the O and B2 of Ti₂AlNb intermetallic: A first principles study K Goyal, N Sardana - <i>Journal of Physics and Chemistry of Solids</i>, 2023</p> <p>Abstract: The intermetallic stability, structural, and elastic properties of the B2 and the O intermetallic of Ti₂AlNb intermetallic doped with IVB, VB, and VIB elements of the periodic table are studied using density functional theory. The energy of formation and calculated elastic constants reveal that all the doped intermetallics are thermodynamically and mechanically stable. The derived elastic moduli and Pugh's ratio confirm that doping with quaternary elements can enhance the mechanical properties and ductility of the Ti₂AlNb intermetallic in both the B2 and the O intermetallic. Further, elements that enhance the ductility and hardness in the O intermetallic, decrease the same in the B2 intermetallic. Among all the systems, Mo and W provide the most enhancement in <i>B</i>, <i>G</i>, and <i>E</i> values in both the B2 and O intermetallic. Ductility of the B2 intermetallic is most enhanced by Ti and Nb while of the O intermetallic by Cr and Mo. All the dopants increase the melting point where W provides the most enhancement. Poisson's ratio, hardness, and Cauchy pressures are further investigated. The electronic density of states indicates that dopants induce redistribution of charge due to new bond formations resulting to a significant change in intermetallic stability and mechanical properties.</p>
27.	<p>Effect of water hyacinth (<i>Eichhornia crassipes</i>) plant into water bodies and its composite materials for commercial applications A Arivendan, WJJ Thangiah, R Das, D Ahamad... - <i>Proceedings of the Institution of Mechanical Engineers, Part C: Journal of Mechanical Engineering Science</i>, 2023</p> <p>Abstract: Water Hyacinth (<i>Eichhornia crassipes</i>) is a free-floating aquatic plant that is commonly found in local water bodies. Its quick emergence and rapid expansion are the main advantages, allowing it to cover entire water surfaces. The government considers the plant to be waste and has invested a significant amount of money to remove it from water bodies. This paper provides a brief overview of the effective use of water hyacinth in wastewater treatment, converting it into WH fiber. By utilizing the water hyacinth fiber and an epoxy matrix, a WH composite is produced. The hyacinth fiber reinforced composite samples attained 27.06 MPa tensile strength and 43.51 MPa flexural strength, and 1.25 J impact strength. Water hyacinth plant presented water bodies water level parameters are tested with the help of the suitcase method. Essential tests, such as mechanical testing, thermal behavior, and characterization techniques (XRD, FTIR, SEM, optical microscope inspection, and water and chemical absorption tests), are conducted. In conclusion, the results suggest that the water hyacinth plant could be better utilized in the production of commercial household applications and lightweight materials in the field of natural fiber composites.</p>
28.	<p>Electrocatalytic performance of green synthesized nitrogen-doped carbon dots toward clean energy H₂ generation N Selvaraju, J Murugan, S Selvaraj, N Singhal, G Venugopal - <i>Materials Letters</i>, 2023</p> <p>Abstract: Non-metal carbonaceous and elemental doping are efficient methods for improving the electrocatalytic activity of the hydrogen evolution reaction (HER). Nitrogen-doped carbon quantum dots were produced under various conditions and operate exceptionally well in an acidic environment. The results of the experiments show that nitrogen doping improved hydrogen adsorption and accelerated HER kinetics. It demonstrates higher performance with an</p>

overpotential of -0.268 V due to doping, which indirectly lowered electron-hole pair recombination as evidenced by time-constant estimation, as well as outstanding stability. This research will provide a viable platinum-free material that may be used as an effective electrocatalyst for the HER reaction.

Graphical abstract:



[Enhancement in the limit of detection of lab-on-chip microfluidic devices using functional nanomaterials](#)

V Vaishampayan, A Kapoor, SP Gumfekar - The Canadian Journal of Chemical Engineering, 2023

29.

Abstract: Technological developments in recent years have witnessed a paradigm shift towards lab-on-chip devices for various diagnostic applications. Lab-on-chip technology integrates several functions typically performed in a large-scale analytical laboratory on a small-scale platform. These devices are more than the miniaturized versions of conventional analytical and diagnostic techniques. The advances in fabrication techniques, material sciences, surface modification strategies, and their integration with microfluidics and chemical and biological-based detection mechanisms have enormously enhanced the capabilities of these devices. The minuscule sample and reagent requirements, capillary-driven pump-free flows, faster transport phenomena, and ease of integration with various signal readout mechanisms make these platforms apt for use in resource-limited settings, especially in developing and underdeveloped parts of the world. The microfluidic lab-on-a-chip technology offers a promising approach to developing cost-effective and sustainable point-of-care testing applications. Numerous merits of this technology have attracted the attention of researchers to develop low-cost and rapid diagnostic platforms in human healthcare, veterinary medicine, food quality testing, and environmental monitoring. However, one of the major challenges associated with these devices is their limited sensitivity or the limit of detection. The use of functional nanomaterials in lab-on-chip microfluidic devices can improve the limit of detection by enhancing the signal-to-noise ratio, increasing the capture efficiency, and providing capabilities for devising novel detection schemes. This review presents an overview of state-of-the-art techniques for integrating functional nanomaterials with microfluidic devices and discusses the potential applications of these devices in various fields.

30.

[Entropy based spectral clustering for distribution network with high penetration of dgs](#)

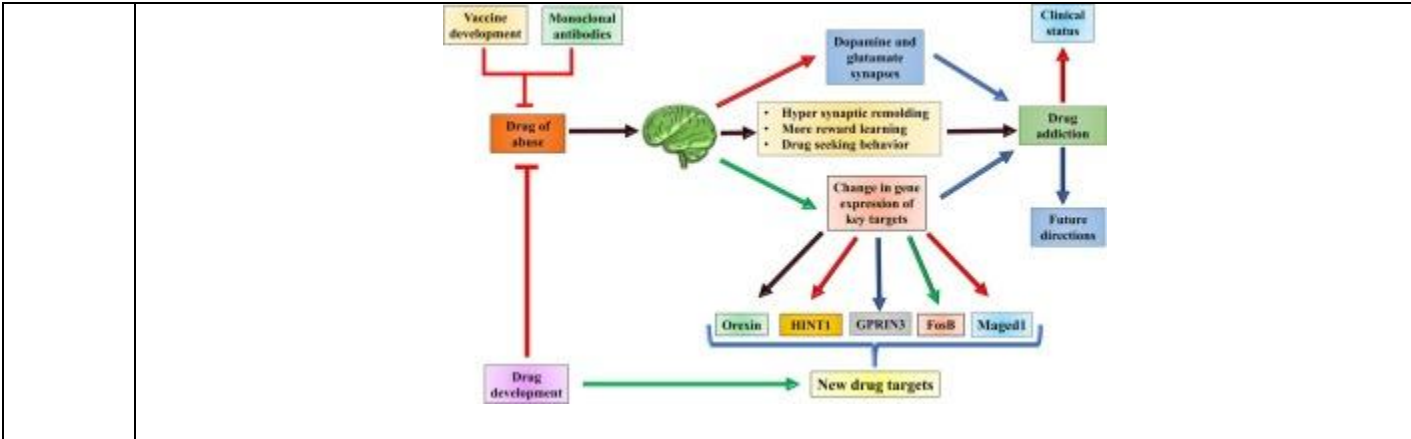
D Kumar, BP Padhy - 22nd National Power Systems Conference (NPSC), 2023

Abstract: High penetration of distributed generation (DG) into the distribution network (DN) causes voltage limit violation at several buses. With the evolution in inverter technology, DGs offer an optimistic solution to maintain the voltage profile by controlling its active and reactive power. Centralized voltage control (CVC) using the voltage controlling capability of available DGs in the distribution network is not a good solution due to the size of the DN. Additionally, perturbation at any DGs does not impact the voltage level at all buses equally. For maintaining the voltage profile at a few buses, power curtailment from all the DGs is not an economically fair

	<p>solution for the utility grid. Therefore, decentralized voltage control is considered as a more practical and economical approach to maintaining the voltage profile at all buses. In this paper, novel entropy-based spectral clustering has been proposed to partition the DN. For implementing the proposed method, the impact of DGs on voltage deviation has been measured in terms of entropy. Further using entropy, spectral clustering has been performed. The proposed clustering decouples the distribution network in such a way that available DGs in clusters are capable of maintaining voltage profiles in the clusters. Further effectiveness of the proposed method has been done on IEEE 33 test system.</p>
31.	<p>Estimation of defect depth in carbon fibre reinforced polymer using frequency modulated thermal wave imaging: an analytical study A Rani, P Das, A Sharma... - Russian Journal of Nondestructive Testing, 2023</p> <p>Abstract: Frequency modulated thermal wave imaging (FMTWI) is an efficient and affective thermal nondestructive testing and evaluation (NDT&E) technique for qualitative and quantitative analysis for defects in test materials. FMTWI utilizes low peak power heat sources modulated within a frequency sweep to excite the material under test. The paper demonstrates a novel analytical approach for heat diffusion in isotropic material using FMTWI technique to distinguish defects located at different depths inside the test sample. The frequency modulated thermal excitation has been illuminated over carbon fibre reinforced polymer (CFRP) material to compute thermal response over the object under test. The mapped temperature response is analysed further for defect detectability in terms of correlation coefficient and time delay. Further, the presented analytical approach for defects located at different depths are compared with the simulation model of CFRP test material. Lastly, different frequency and time domain data analysis schemes have been applied to detect defects in terms of thermal contrast. Results demonstrates the detection capability of FMTWI technique using correlation based matched filter method to provide better test resolution and sensitivity.</p>
32.	<p>Experimental demonstration on suppression of viscous fingering in a partially miscible system K Iwasaki, Y Nagatsu, T Ban, J Iijima, M Mishra... - Physical Chemistry Chemical Physics, 2023</p> <p>Abstract: Phase separation is ubiquitous in nature and technology. So far, the focus has primarily been on phase separation occurring in the bulk phase. Recently, phase separation taking place in interfacial areas has been attracting attention, particularly, a combination of interfacial phase separation and hydrodynamics. Studies on this combination have been conducted intensely in this decade; however, the detailed dynamics are still not clear. Here, we perform fluid displacement experiments, where a less viscous solution displaces a more viscous one in a radial confined geometry and phase separation occurs at the interfacial region. We demonstrate that a finger-like pattern because of the viscosity contrast during the displacement can be suppressed by the phase separation. We also claim that the direction of a body force, the so-called Korteweg force, which appears during the phase separation and induces convection, determines whether the fingering pattern is suppressed or the fingering pattern is changed to a droplet pattern. The change from the fingering pattern to the droplet pattern is enhanced by the Korteweg force directed from the less viscous solution to the more viscous one, while the fingering is suppressed by the force directed in the opposite direction. These findings will contribute directly to the higher efficiency of processes such as enhanced oil recovery and CO₂ sequestration, where interfacial phase separation is considered to occur during the flow.</p>
33.	<p>Experimental investigation of a low-cost humidification-dehumidification desalination cycle using packed-bed humidifier and finned-tube heat exchanger K Garg, R Beniwal, SK Das, H Tyagi - Thermal Science and Engineering Progress, 2023</p> <p>Abstract: Humidification-Dehumidification (HDH) desalination technology can ensure adequate freshwater supply to the people living in water-stressed regions in remote locations. Although,</p>

	<p>HDH process can be operated by using simple and inexpensive components such as cooling tower and heat exchanger which are readily available in the market. But to achieve the desired freshwater productivity and thermal performance, it is important to carry out the detailed design of these components and choose the right operating parameters such as mass flow rate ratio, top brine temperature which significantly affects system performance. In the present study, the thermal performance of a closed-air, open-water and water-heated version of the HDH cycle has been investigated experimentally and the previously developed detailed numerical model for the similar HDH cycle has been validated with the experimental results. The HDH system has been built with a counter-flow packed-bed cooling tower and finned-tube heat exchangers which are widely utilized across all industries. The thermal performance of the system is evaluated in terms of four main parameters which are gained output ratio (GOR), distillate flow rate, and the effectiveness of the humidifier as well as the dehumidifier by varying the top brine temperature as well as the mass flow rate ratio. It is observed that the present system can produce around 125.5 L of freshwater per day, having total dissolved solids of approximately less than 15 ppm, operating at a feed temperature of only 61.7 °C and mass flow rate ratio (MR) of 2.34. At these operating conditions, energy effectiveness of the humidifier and dehumidifier were approximately 0.75 and 0.80. The gained output ratio (GOR) of the present system is quite modest (=0.81) which indicates that the system may be further improved in the future. The results of our current experimental study validated the predictions of the model developed in our prior study. Hence, the model can be utilized to design the HDH system as per the desired output of freshwater and GOR. The results from both experiments and simulations are in closer agreement with each other. The numerical analysis also showed that the integration of solar energy-driven AHT (Absorption Heat Transformer) has the potential to further increase the production rate of the HDH system. The economic performance of the system revealed the leveled cost of water production (LCOW) from such a system is approximately USD 4.0 $\\$/\text{m}^3$ of fresh water but the total capital expenditure to install this system is very low (<USD \$1500). Overall, it was inferred that an HDH system with optimum performance can be designed and installed at a much lower cost, and using simple construction, which is a huge advantage for marginalized communities living in remote locations across the world (since the simple components of this system can be easily operated and maintained by them).</p>
34.	<p><u>Evading tipping points in socio-mutualistic networks via structure mediated optimal strategy</u> S Deb, S Bhandary, PS Dutta - <i>Journal of Theoretical Biology</i>, 2023</p> <p>Abstract: The threat of large-scale pollinator decline is increasing globally under stress from multiple anthropogenic pressures. Traditional approaches have focused on managing endangered species at an individual level, in which the effect of complex interactions such as mutualism and competition are amiss. Here, we develop a coupled socio-mutualistic network model that captures the change in pollinator dynamics with human conservation opinion in a deteriorating environment. We show that the application of social norm (or conservation) at the pollinator nodes is fit to prevent sudden community collapse in representative networks of varied topology. Whilst primitive strategies have focused on regulating abundance as a mitigation strategy, the role of network structure has been largely overlooked. Here, we develop a novel network structure-mediated conservation strategy to find the optimal set of nodes on which norm implementation successfully prevents community collapse. We find that networks of intermediate nestedness require conservation at a minimum number of nodes to prevent a community collapse. We claim the robustness of the optimal conservation strategy (OCS) after validation on several simulated and empirical networks of varied complexity against a broad range of system parameters. Dynamical analysis of the reduced model shows that incorporating social norms allows the pollinator abundance to grow that would have otherwise crossed a tipping point and undergo extinction. Together, this novel means OCS provides a potential plan of action for conserving plant-pollinator networks bridging the gap between research in mutualistic networks and conservation ecology.</p>

35.	<p>Free convection from a vertical plate to generalized Newtonian fluids K Aherwar, AH Raja, SAPatel, RP Chhabra - <i>Journal of Non-Newtonian Fluid Mechanics</i>, 2023</p> <p>Abstract: Laminar free convective heat transfer to power-law and Bingham plastic fluids from a vertical surface has been studied numerically. New extensive results for streamlines, isotherms, local and surface-averaged Nusselt number presented herein embrace the following ranges of conditions: $0.2 \leq n \leq 1$; $1 \leq \text{PrPL} \leq 100$; $10 \leq \text{GrPL} \leq 10^5$ for power-law fluids and $1 \leq \text{Bn} \leq \text{Bnmax}$, $10 \leq \text{PrBP} \leq 100$ and $10^2 \leq \text{RaBP} \leq 10^5$ for Bingham plastics. The effect of the two thermal conditions on the plate, namely, constant temperature (CWT) and constant heat flux (CHF) has also been investigated. Otherwise, under identical conditions, shear-thinning fluid viscosity facilitates overall heat transfer by up to 80–100% over and above that in Newtonian fluids. On the other hand, Bingham yield stress adversely influences heat transfer due to the formation of unyielded domains thereby leading to changes in temperature gradients on the surface of the plate. Beyond a critical Bingham number, conduction is the sole mode of heat transfer. The values of the average Nusselt number have been consolidated in the form of a modified Rayleigh number for power-law liquids. These results also help delineate the conditions for the onset of convection as well as the limits of the Boundary-layer flow approximation. For Bingham plastics, the average Nusselt number decreases gradually with the increasing ratio of the yield stress and the buoyancy-induced forces approaching the conduction limit at about $\text{Bn}/\text{Gr}_{\text{BP}}^{1/2} \sim 1-2$.</p>
36.	<p>Future perspectives of emerging novel drug targets and immunotherapies to control drug addiction JA Malik, JN Agrewala - <i>International Immunopharmacology</i>, 2023</p> <p>Abstract: Substance Use Disorder (SUD) is one of the major mental illnesses that is terrifically intensifying worldwide. It is becoming overwhelming due to limited options for treatment. The complexity of addiction disorders is the main impediment to understanding the pathophysiology of the illness. Hence, unveiling the complexity of the brain through basic research, identification of novel signaling pathways, the discovery of new drug targets, and advancement in cutting-edge technologies will help control this disorder. Additionally, there is a great hope of controlling the SUDs through immunotherapeutic measures like therapeutic antibodies and vaccines. Vaccines have played a cardinal role in eliminating many diseases like polio, measles, and smallpox. Further, vaccines have controlled many diseases like cholera, dengue, diphtheria, Haemophilus influenza type b (Hib), human papillomavirus, influenza, Japanese encephalitis, etc. Recently, COVID-19 was controlled in many countries by vaccination. Currently, continuous effort is done to develop vaccines against nicotine, cocaine, morphine, methamphetamine, and heroin. Antibody therapy against SUDs is another important area where serious attention is required. Antibodies have contributed substantially against many serious diseases like diphtheria, rabies, Crohn's disease, asthma, rheumatoid arthritis, and bladder cancer. Antibody therapy is gaining immense momentum due to its success rate in cancer treatment. Furthermore, enormous advancement has been made in antibody therapy due to the generation of high-efficiency humanized antibodies with a long half-life. The advantage of antibody therapy is its instant outcome. This article's main highlight is discussing the drug targets of SUDs and their associated mechanisms. Importantly, we have also discussed the scope of prophylactic measures to eliminate drug dependence.</p> <p>Graphical abstract:</p>



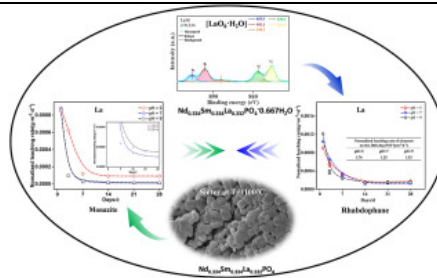
37. [Headroom based Frequency and DC-Voltage Control for Large Disturbances in Multi-Terminal HVDC \(MTDC\) Grids](#)
 AS Kumar, BP Padhy - IEEE International Conference on Power Electronics, Drives and Energy Systems (PEDES), 2023

Abstract: In the AC integrated Multi-terminal HVDC (AC-MTDC) grids, it is indispensable to regulate the DC-voltage and frequency for reliable and stable operation. For effective DC-voltage and frequency regulation, Headroom-based Adaptive Droop Control (HR-ADC) has been proposed in this paper. The HR-ADC changes the droop value adaptively based on the available headroom at Grid Side Voltage Source Converter (GSC), and available power at the Wind or Solar Farms while operating Renewable Source side VSC (RSC). This approach is robust and ensures system stable operation and reliability even during significant disturbances in the AC-MTDC grids. The proposed method is validated by considering two case studies in PSCAD/EMTDC simulation of the five terminal CIGRE Bipolar DC grid benchmark model integrated into two area power systems.

38. [Homogeneous immobilization of simulated actinides in rhabdophane and comparison of its leaching stability with monazite](#)
 Q Zheng, X Zhao, Y Liu...R Ahuja - Progress in Nuclear Energy, 2023

Abstract: Rhabdophane $\text{LnPO}_4 \cdot 0.667\text{H}_2\text{O}$ ($\text{Ln} = \text{La}$ to Dy) is an important precipitation-enrichment barrier to isolate actinides from groundwater. However, the bearing capacity of different actinides in rhabdophane has been poorly understood due to the complex coordination environment induced by water molecules. In this work, the precipitation behaviors of $\text{Nd}_x\text{Sm}_x\text{La}_{1-2x}\text{PO}_4 \cdot 0.667\text{H}_2\text{O}$ ($x = 0.1-0.5$) solid solutions are systematically investigated to understand the simulated actinides occupancy and the chemical precipitation processes. The results show that Nd^{3+} and Sm^{3+} can be removed over 99% after 12 h in an approximate $\text{pH} = 1$ solution. $\text{Nd}_x\text{Sm}_x\text{La}_{1-2x}\text{PO}_4 \cdot 0.667\text{H}_2\text{O}$ single-phase has been observed by refined XRD, although the composition distribution of nanograins is extremely uneven. The distribution of simulated actinides can be homogeneous after prolonging reaction time to 12 days or sintering temperature over 1000°C . Both Nd^{3+} and Sm^{3+} are preferentially incorporated on non-hydrated lattice sites when $x \leq 0.1$. Besides, the chemical stability of $\text{La}_{0.332}\text{Nd}_{0.334}\text{Sm}_{0.334}\text{PO}_4 \cdot 0.667\text{H}_2\text{O}$ rhabdophane is compared with associated monazite to understand the leaching activities of simulated actinides incorporated on hydrated and non-hydrated sites. The leaching rates of monazite are smaller than that of rhabdophane, suggesting that $[\text{LnO}_9]$ polyhedrons in monazite have a stronger energy threshold than $[\text{LnO}_8]$ and $[\text{LnO}_8 \cdot \text{H}_2\text{O}]$ polyhedrons in rhabdophane.

Graphical abstract:

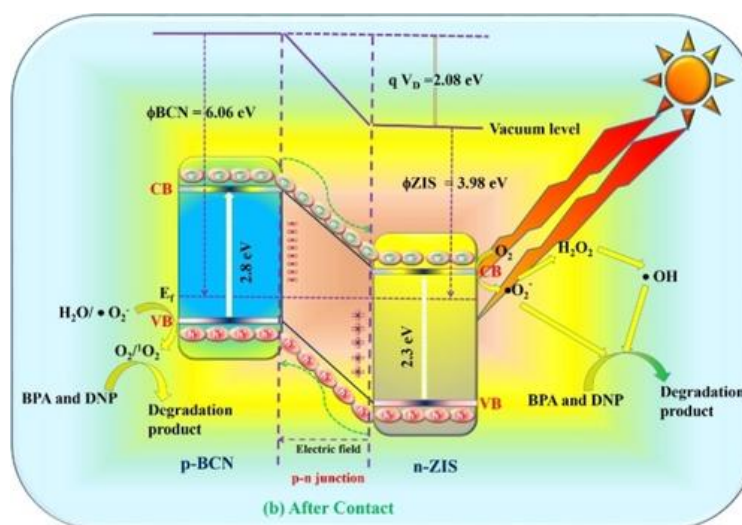


39.	<p>Impact of exchange rate on trade balance of india: evidence from threshold cointegration with asymmetric error correction approach L Mallick, SR Behera, M Bhattacharya - Foreign Trade Review, 2023</p> <p>Abstract: In this research, we investigate the dynamic relationship between the trade balance and exchange rate in the case of India using threshold cointegration and an asymmetric error-correction model. Empirical results validate that the long-run dynamic relationship between the trade balance and exchange rates is asymmetric. In the short run, the trade balance responds only due to positive deviations in the exchange rate. In contrast, in the exchange rate model, the exchange rate reacts only due to negative deviations in the trade balance. In addition, the results exhibit that the adjustment following variation in the exchange rate seems higher than the adjustment in the trade balance in the short run. Besides, the results indicate that the speed of adjustment due to the positive and negative shocks differs in the trade balance and the exchange rate models. Further, the uni- directional Granger causality result suggests that the trade balance substantially affects the exchange rate. However, the Granger causality effect of the exchange rate on the trade balance seems minimal. Finally, our results validate the impact of momentum equilibrium adjustment path asymmetric effects between the trade balance and exchange rate, indicating that the adjustment path is asymmetric in the long run. Therefore, policy planners in India should consider the asymmetric adjustment between these two drivers to overcome trade balance discrepancies in the short and long run.</p>
40.	<p>Implementation of gold and silver nanoparticles in sensing and bioengineering G Bhardwaj, N Kaur, N Singh - Gold and Silver Nanoparticles: A Book Chapter, 2023</p> <p>Abstract: In the era of nanotechnology, nanoparticles are considerably studied as chemosensors and biosensors because of their excellent performance in terms of sensitivity, selectivity, linearity, stability, response time, and reproducibility. These nanoparticles are generally reduced metal (gold/silver) salts in fluid usually water, which provide vibrant colors with the interaction of light. The metallic nanoparticles exhibit unique traits of changing their physical, chemical, and biological properties by changing their surface-to-volume ratio: therefore, can be used for various modifications and applications. Among various metallic nanoparticles, noble metal nanoparticles are the most captivating and vivacious nanoparticles in field of applications. Some unique properties such as biocompatibility, conductivity, high density, and high surface-to-volume ratio facilitate the use of gold and silver nanoparticles in sensing. The similarity with the size of biological molecules enhances the potential use of gold and silver nanoparticles in sensing, biosensing, and medicines. Whilst the capability of gold nanoparticles to cross the blood-brain barrier to interact with DNA facilitates their use in biomedicine. Large surface area and tendency to get coated with many kinds of organic and inorganic molecules manifest their use in drug delivery systems with great efficiency. These properties lead to a broad range of applications in the field of organic photovoltaics, sensing, therapeutic agents, drug delivery, bioengineering, and many more. This book chapter focuses on the recent reports of sensing and bioengineering application of gold and silver nanoparticles.</p>
41.	<p>Improving the segmentation of digital images by using a modified Otsu's between-class variance S Singh, N Mittal, H Singh, D Oliva - Multimedia Tools and Applications, 2023</p>

	<p>Abstract: Image segmentation is a critical stage in the analysis and pre-processing of images. It comprises dividing the pixels according to threshold values into several segments depending on their intensity levels. Selecting the best threshold values is the most challenging task in segmentation. Because of their simplicity, resilience, reduced convergence time, and accuracy, standard multi-level thresholding (MT) approaches are more effective than bi-level thresholding methods. With increasing thresholds, computer complexity grows exponentially. A considerable number of metaheuristics were used to optimize these problems. One of the best image segmentation methods is Otsu's between-class variance. It maximizes the between-class variance to determine image threshold values. In this manuscript, a new modified Otsu function is proposed that hybridizes the concept of Otsu's between class variance and Kapur's entropy. For Kapur's entropy, a threshold value of an image is selected by maximizing the entropy of the object and background pixels. The proposed modified Otsu technique combines the ability to find an optimal threshold that maximizes the overall entropy from Kapur's and the maximum variance value of the different classes from Otsu. The novelty of the proposal is the merging of two methodologies. Clearly, Otsu's variance could be improved since the entropy (Kapur) is a method used to verify the uncertainty of a set of information. This paper applies the proposed technique over a set of images with diverse histograms, which are taken from Berkeley Segmentation Data Set 500 (BSDS500). For the search capability of the segmentation methodology, the Arithmetic Optimization algorithm (AOA), the Hybrid Dragonfly algorithm, and Firefly Algorithm (HDAFA) are employed. The proposed approach is compared with the existing state-of-art objective function of Otsu and Kapur. Qualitative experimental outcomes demonstrate that modified Otsu is highly efficient in terms of performance metrics such as PSNR, mean, threshold values, number of iterations taken to converge, and image segmentation quality.</p>
42.	<p><u>Incorporating the climate oscillations in the computation of meteorological drought over India</u> DC Naik, SR Chavan, P Sonali - Natural Hazards, 2023</p> <p>Abstract: Large-scale climate oscillations (e.g. Nino 3.4, SOI, MEI and IOD) govern the occurrence of meteorological droughts. The present study is envisaged to model non-stationary meteorological drought index, at the grid scale covering entire India by considering the large-scale climate oscillations affecting the phenomenon of precipitation. The non-stationary framework is considered to estimate the Standardized Precipitation Index (SPI), which in turn is used for analysing the frequency of severe and extreme drought events for two reference time periods (i.e. 1901–1950 and 1951–2018) at various timescales, viz. 3, 6, 9 and 12 months. The efficiency of non-stationary SPI (NSPI) approach over stationary SPI (SSPI) approach in characterizing the drought events is evaluated based on two precipitation datasets from the India Meteorological Department (IMD) and Climate Research Unit (CRU). The NSPI is observed to outperform the SSPI in assessing the meteorological droughts at majority of the grids over India as the timescale increases from 3 to 12 months. Different sets of climate oscillations with significant correlation with precipitation are identified for IMD and CRU datasets as well as for different reference periods, indicating that the drought characterization is sensitive to the chosen reference time period as well as the precipitation datasets considered for the analysis. Overall the NSPI approach is shown to provide reliable and robust determination of drought characteristics by incorporating the climate oscillations under changing climate. The findings from this study can be used to devise adaptation strategies to mitigate adverse impacts of droughts.</p>
43.	<p><u>Interfacial charge transfer of b-doped g-C₃N₄/ZnIn₂S₄ p-n heterojunction for plasticizer bisphenol-a and dye/drug intermediates, 2,4-dinitrophenol degradation in sunlight</u> A Behera, A Ghoshal, R Srivastava - ChemistrySelect, 2023</p> <p>Abstract: Fabricating an efficient photocatalyst for solving energy and environmental pollution is challenging, especially using sunlight. Herein, a photocatalyst was developed to degrade</p>

plasticizer (Bisphenol A, BPA) and an industrial-pollutant 2,4-dinitrophenol (DNP) found in water bodies with sunlight. Several $\text{ZnIn}_2\text{S}_4/\text{B}$ -doped $\text{g-C}_3\text{N}_4$ (ZIS@BCN) heterojunctions were prepared by an ultra-sonochemical route followed by calcination. HRTEM, MS analysis, EIS, photocurrent, and synergic factor calculations were employed to confirm p-n heterojunction. The phase purity and optical characteristics of the photocatalysts were determined by XRD, PL, and DRS UV-Vis spectroscopy. A successful p-n heterojunction 2% ZIS@BCN showed better degradation efficiency than pristine ZIS (n-type) and BCN (p-type) semiconductors. Moreover, the best photocatalyst (2% ZIS@BCN) exhibited maximum photo-degradation of 83% of BPA and 85% of DNP under solar light illumination. The degradation pathways and involvement of reactive species were confirmed using LC-MS, trapping experiments, nitroblue-tetrazolium, and terephthalic acid tests. The superior activity is ascribed to the successful formation of an electrical double layer (EDL) between p-type BCN and n-type ZIS, which minimizes the e^-h^+ recombination and thereby increases the visible light utilization efficiency. The work validates the formation of ZIS@BCN p-n heterojunction, showing solar light-driven photocatalytic degradation of toxic effluents found in water bodies.

Graphical abstract:

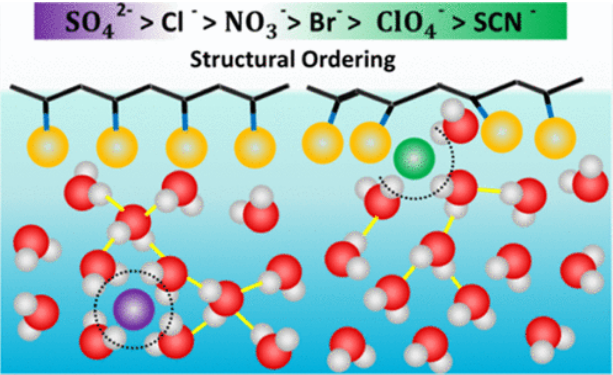


$\text{ZnIn}_2\text{S}_4/\text{B}$ -doped $\text{g-C}_3\text{N}_4$ exhibited excellent photocatalytic activity to degrade plasticizer Bisphenol A, and an industrial-pollutant 2,4-dinitrophenol found in water bodies with sunlight due to the successful formation of an electrical double layer between p-type BCN and n-type ZIS, which minimize the e^-h^+ recombination and thereby increases the visible light utilization efficiency.

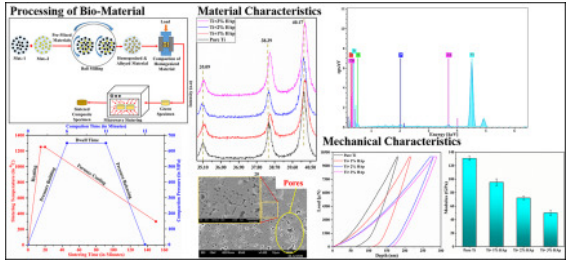
[Investigating the tail behaviour and associated risk with daily discharges in South Indian Rivers](#)
 N Gupta, SR Chavan - Stochastic Environmental Research and Risk Assessment, 2023

44.

Abstract: The adequate choice of a distribution that can fit a dataset, especially to its right tail (large extreme events), is a major problem in flood frequency analysis. Decision support systems (DSS) have been used in the past to define the appropriate class of distribution based on the tail behaviour of the data before its model selection. This paper investigates the tail behaviour of probability distribution of the daily streamflow data in south Indian rivers and also assesses the information related to tail risk, as it has many practical and societal consequences. In this paper, we apply and compare two DSS, (i) given by Martel et al. (J Hydrol Eng 18(1):1–9, 2013) and (ii) concentration profile–concentration adjusted expected shortfall (CP–CAES) based DSS, along with some newly developed graphical diagnostic tools, such as CP, CAES, discriminant moment ratio plot, maximum-to-sum plot, and Zenga plot to characterize the tails of probability distributions into an appropriate class. Further, the tail risk is analyzed using a novel risk

	<p>management approach known as a concentration map (CM), which makes use of the concentration profiles of daily streamflow datasets. Results indicate that the proposed DSS is a potential tool for tail characterization. The study suggests the use of heavy-tailed distributions to model daily streamflow data over south Indian catchments. Neglecting heavy-tailed distributions, when found appropriate, can lead to an underestimation of the likelihood of floods and has catastrophic consequences for risk. CM is found suitable for assessing the tail risk associated with the daily streamflow dataset, which inherently represents the frequency and magnitude of extreme floods.</p>
45.	<p>Ion-specific water–macromolecule interactions at the air/aqueous interface: an insight into hofmeister effect B Rana, DJ Fairhurst, KC Jena - Journal of the American Chemical Society, 2023</p> <p>Abstract: The specificity of ions in inducing conformational changes in macromolecules is introduced as the Hofmeister series; however, the detailed underlying mechanism is not comprehensible yet. We utilized surface-specific sum frequency generation (SFG) vibrational spectroscopy to explore the Hofmeister effect at the air/polyvinylpyrrolidone (PVP)/water interface. The spectral signature observed from the ssp polarization scheme reveals ion-specific ordering of water molecules following the Hofmeister series attributed to the ion–macromolecule interactions. Along with this, the presence of ions does not reflect any significant influence on the structure of the PVP macromolecule. However, the ppp-SFG spectra in the CH-stretch region reveal the impact of ions on the orientation angle of vinyl chain CH₂-groups, which follows the Hofmeister series: SO₄²⁻ > Cl⁻ > NO₃⁻ > Br⁻ > ClO₄⁻ > SCN⁻. The minimal orientation angle of CH₂-groups indicates significant reordering in PVP vinyl chains in the presence of chaotropic anions ClO₄⁻, and SCN⁻. The observation is attributed to the ion-specific water–macromolecule interactions at the air/aqueous interface. It is compelling to observe the signature of spectral blue shifts in the OH-stretch region in the ppp configuration in the presence of chaotropic anions. The origin of spectral blue shifts has been ascribed to the existence of weaker interactions between the interfacial water molecules and the backbone CH- and CH₂-moieties of the PVP macromolecules. The ion-specific modulation in water–macromolecule interactions is endorsed by the relative propensity of anion’s adsorption toward the air/aqueous interface. The experimental findings highlight the existence and cooperative participation of ion-specific water–macromolecule interactions in the mechanism of the Hofmeister effect, along with the illustrious ion–water and ion–macromolecule interactions.</p> 
46.	<p>Ketamine-Induced Ego Dissolution is Related to the Functional Connectivity Reconfiguration of the Posteromedial Cortex M Li, N Sharma, L Danyeli, L Colic, N Opel, T Chand...D Bathula... - Biological Psychiatry, 2023</p> <p>Abstract: A single dose of intravenous ketamine improves the severity of symptoms in disorders</p>

	<p>such as depression while also introducing acute and transient ego dissolution during administration. Understanding the neural correlates of ego dissolution may help elucidate its therapeutic effect mechanism. Previous studies suggested that the posteromedial cortex (PMC) activity is related to the altered sense of self and the sense of dissociation, phenomena underlying ego dissolution.</p>
47.	<p>Leakage current measurement in ldpe under dc polarity reversal stress C Iyyapan, CC Reddy - IEEE 6th International Conference on Condition Assessment Techniques in Electrical Systems (CATCON), 2023</p> <p>Abstract: Insulation material performance is severely impacted by the HVDC polarity reversal (PR), and life estimation models demonstrate that LDPE under short reversal time interval failed quickly as compared to higher intervals. This difference in breakdown time is explored in relation with LDPE leakage current characteristics. The experiments were performed in a 30μm sample under 200 kV/mm electric field of 1 minute and 10 minute reversal. An ammeter hardware setup is used to measure the current until breakdown. The continuously measured current of each reversal interval was sequentially split into three sections and compared. Significant difference in instantaneous polarization and relaxation current was observed. Also, dissimilar leakage current trend in 1 minute and 10 minute tests was observed, and these results were correlated with the charge dynamics in LDPE to explain the variations in the breakdown.</p>
48.	<p>Location specific multi-scale characterization and constitutive modeling of pig aorta KK Dwivedi, P Lakhani, A Yadav, Deepak, S Kumar, N Kumar - Journal of the Mechanical Behavior of Biomedical Materials, 2023</p> <p>Abstract: The mechanical and structural behavior of the aorta depend on physiological functions and vary from proximal to distal. Understanding the relation between regionally varying mechanical and multi-scale structural response of aorta can be helpful to assess the disease outcomes. Therefore, this study investigated the variation in mechanical and multi-scale structural properties among the major segments of aorta such as ascending aorta (AA), descending aorta (DA) and abdominal aorta (ABA), and established a relation between mechanical and multi-structural parameters. The obtained results showed significant increase in anisotropy and nonlinearity from proximal to distal aorta. The change in periphery length and radii between load and stress free configuration was also found increasing far from the heart. Opening angle was significantly large for ABA than AA and DA (AA/DA vs ABA; $p = 0.001$). Mean circumferential residual stretch (ratio of mean periphery length at load and stress free configurations) was found decreasing between AA and DA, and then increasing between DA to ABA and its value was significantly more for ABA (AA vs DA; $p = 0.041$, AA vs ABA; $p = 0.001$, DA vs ABA; $p = 0.001$). The waviness of collagen fibers, collagen fiber content, collagen fibril diameter and total protein content were found significantly increasing from proximal to distal. Pearson correlation test showed a significant linear correlation between variation in mechanical and multi-scale structural parameters over the aortic length. Residual stretch was found positively correlated with collagen fiber content ($r = 0.82$) whereas opening angel was found positively correlated with total protein content (TPC) ($r = 0.76$).</p>
49.	<p>Measuring ideation effectiveness in bioinspired design S Sharma, S Gururani, P Sarkar - AI EDAM, 2023</p> <p>Abstract: Analogies provide better concept generation in engineering design. This ideation can be measured by metrics such as usefulness, novelty, variety, quality, completeness, and quantity. In bioinspired design, biological analogies are used to inspire design concepts. Biological analogies have been provided in earlier studies to measure ideation effectiveness. Tools like IDEA-INSPIRE, DANE, etc., allow designers to search analogies using functions, behaviors, and structures. However, we wanted to inquire about the effect of providing a very large number of biological analogies (26), fulfilling the same function to develop bioinspired solutions. In this</p>

	<p>paper, an empirical study has been performed to analyze the effect of biological analogies on ideation. The designers are exposed to provided multiple biological analogies and generate concepts for which four ideation metrics: novelty, variety, quality, and quantity metrics are evaluated. The results are compared to the unaided condition where other designers are given the same task. A new method to measure variety using a 2D matrix has been presented. The results suggest that designers can generate bioinspired solutions when multiple biological analogies performing similar functions are provided in a presentable format. Statistically, exposure to multiple biological analogies in idea generation can significantly increase the variety of design ideas. The novelty, quality, and quantity for the biological group and control group remain the same.</p>
50.	<p><u>Micro-hydroxyapatite reinforced Ti-based composite with tailored characteristics to minimize stress-shielding impact in bio-implant applications</u> R Kumar, A Agrawal - <i>Journal of the Mechanical Behavior of Biomedical Materials</i>, 2023</p> <p>Abstract: Biomaterials having higher strength and increased bioactivity are widely researched topics in the area of scaffold and implant fabrication. Metal-based biomaterials are favorably suitable for load-bearing implants due to their outstanding mechanical and structural properties. The issue with pure metallic material used for bio-implant is the mismatch between the mechanical properties of the human body parts and the implant. The mismatch in modulus and hardness values causes damage to muscles and other body parts due to the phenomena of ‘stress-shielding’. As per the rule of mixture, combining a biocompatible ceramic with metals will not only lower the overall mechanical strength, but will also enhance the composite's bioactivity. In the present work, a Metal-Ceramic composite of Ti and μ-HAp is processed through high-energy mechanical alloying. The μ-HAp powders (in a weight fraction of 1%, 2%, and 3%) were alloyed with Pure Ti powder sintered using microwave hybrid heating (MHH). The homogeneously alloyed materials were inspected for chemical and elemental characteristics using XRD, SEM-EDX, and FTIR analyses. Nano-mechanical and micro-hardness properties were inspected for the fabricated Ti- μ-HAp composites and it shows a decreasing trend. Elastic modulus declined from 130.8 GPa to 50.11 GPa for 3 wt% μ-HAp compared to pure-Ti sample. The mechanical behaviour of developed composites confirms that it can minimize the stress-shielding impact due to comparatively lesser strength and hardness than pure metallic samples.</p> <p>Graphical abstract:</p> 
51.	<p><u>Micro-mechanical insights into the stress transmission in strongly aggregating colloidal gel</u> YAG Man, DS Dagur, S Roy - <i>Journal of Chemical Physics</i>, 2023</p> <p>Abstract: Predicting the mechanical response of soft gel materials under external deformation is of paramount importance in many areas, such as foods, pharmaceuticals, solid–liquid separations, cosmetics, aerogels, and drug delivery. Most of the understanding of the elasticity of gel materials is based on the concept of fractal scaling with very few microscopic insights. Previous experimental observations strongly suggest that the gel material loses the fractal correlations upon deformation and the range of packing fraction up to which the fractal scaling can be applied is very limited. In addition, correctly implementing the fractal modeling requires</p>

	<p>identifying the elastic backbone, which is a formidable task. So far, there is no clear understanding of the gel's elasticity at high packing fractions or the correct length scale that governs its mechanical response. In this work, we undertake extensive numerical simulations to elucidate the different aspects of stress transmission in gel materials. We observe the existence of two percolating networks of compressive and tensile normal forces close to the gel point. We also find that the probability distribution for the compressive and tensile parts normalized by their respective mean shows a universal behavior irrespective of various values of interaction potential and thermal energy and different particle size distributions. Interestingly, there are also a large number of contacts with zero normal force, and, consequently, a peak in the normal force distribution is observed at $fn \approx 0$ even at higher pressures. We also identify the critical internal state parameters, such as the mean normal force, force anisotropies, and the average coordination number, and propose simple constitutive relations that relate different components of stress to internal state parameters. The agreement between our model prediction and the simulation observation is excellent. It is shown that the anisotropy in the force networks gives rise to the normal stress difference in soft gel materials. Our results strongly demonstrate that the mechanical response of the gel system is governed mainly by the particle length scale phenomena, with a complex interplay between the compressive and tensile forces at the particle contact.</p>
52.	<p>Monitoring pollination by honeybee using computer vision V Kujur, AK Bedi, M Saini - International Conference on Intelligent Human Computer Interaction: Part of the Lecture Notes in Computer Science book series, 2023</p> <p>Abstract: Honey bees are critical in pollination worldwide and are essential for crop productivity and ecological management. Knowing more about honeybees and their interaction with plants is urgently needed given the current global pollination crisis. For monitoring pollination, non-invasive approaches are recommended because they diminish the possibility of interfering with pollinator behaviour. Traditional techniques for manually recording pollinator activity in the field can be expensive and time-consuming. In this paper, we have developed a system for pollination monitoring by honeybees using computer vision technique. However, monitoring honeybees is challenging because of their tiny size, swift speed and complex outdoor environments. To detect honeybees in a frame, we have used YOLOv7 as our deep learning model. We have fine-tuned the model on a custom-created dataset for better detection and accuracy. The dataset contains snapshots of YouTube videos in which honeybees were pollinating flowers in different environments. We examined a specific setting where the honeybee pollinated the flowers at several intervals during the video using the detector. We have generated a heatmap and pollination activity graph based on the data from the detector. This information will help with better pollination management, which will increase crop production quality and yield.</p>
53.	<p>Multiobjective approach to schedule dag tasks on voltage frequency islands Sanchit, N Singh, J Singh - IEEE Access, 2023</p> <p>Abstract: Scheduling a Directed Acyclic Graph (DAG) on voltage frequency islands involves dividing the available processing units into multiple islands with varying voltage and frequency levels, and then mapping the tasks of the DAG to the islands while minimizing the makespan and overall energy consumption. In this research work, a novel DAG task scheduling model is introduced with the assistance acquired from the deep learning paradigm. The proposed model includes four major phases: (a) DAG modelling, (b) Voltage frequency island partitioning, (c) core temperature prediction and (d) scheduling optimization. Initially, the Directed Acyclic Graph (DAG) model is designed. The nodes of DAG represent tasks and the edges represent dependencies between tasks. Then, in the Voltage frequency island partitioning, the available processing units into multiple voltage frequency islands. This can be done based on the power consumption of each unit, and the task requirements. Subsequently, the Recurrent Neural</p>

	<p>Network (RERNN) is trained to predict the core temperature of each voltage frequency island based on the multi-objectives like execution time, makespan, overall energy consumption. Then, the scheduling of the DAG on the voltage frequency islands is optimized using the Self-Improved Pelican Optimization Algorithm (SI-POA). The proposed SI-POA model is an extended version of the standard POA model. The SI-POA model is inspired by the behavior by the natural behavior of pelicans during hunting. In the scheduling optimization phase, the SI-POA algorithm to optimize the scheduling of the DAG on the voltage frequency islands while taking into account the predicted core temperature of each island based on the Recalling-enhanced recurrent neural network (RERNN) model. The goal is to minimize the makespan and overall energy consumption of the DAG while keeping the core temperature of each island within safe limits.</p>
54.	<p>Non-adiabatic interactions in $H^+ C_3$ system: An ab initio study P Chahal, TJD Kumar - Chemical Physics, 2023</p> <p>Abstract: Diabatic surfaces generated for the ground state $1^1\Sigma^+(1^1A')$ as well as for the first excited electronic state $2^1\Sigma^+(2^1A')$ have been quantified for the C_3 collision with H^+ system employing the MRCI/aug-cc-pVQZ method. These collisions are significant in understanding the mechanism of energy transfer in astrophysics and molecular physics. For studying the dynamics of the interaction between the charge transfer and inelastic processes, properties such as non-adiabatic coupling matrix elements and mixing angle have been determined. The computed surface and their properties will be useful in studying charge partitioning between the inelastic and charge transfer channels by wave packet quantum dynamics.</p>
55.	<p>Novel texture pattern on WC inserts fabricated using reverse-μEDM for enhanced cutting of Ti6Al4V G Saraf, CK Nirala - Manufacturing Letters, 2023</p> <p>Abstract: Textured rake and flank surfaces of a cutting tool exhibit promising results in machining performances. This work proposes a novel texture pattern to mitigate the disadvantages of the existing textures. Experiments are performed to check the fabrication feasibility of the proposed pattern on the rake face of Tungsten Carbide (WC) inserts using Reverse-micro Electrical Discharge Machining (R-μEDM) process. In order to investigate the advantage of the proposed pattern, orthogonal machining of Titanium alloy is conducted. A significant reduction of 25.77% is obtained in the measured temperature and 11.1% in the friction coefficient compared to the plain insert.</p>
56.	<p>Numerical simulation of shear wave propagation through jointed rocks R Sebastian, K Saha - Proceedings of the 5th International Conference on Numerical Modelling in Engineering: Part of the Lecture Notes in Mechanical Engineering book series, 2023</p> <p>Abstract: Shear wave propagation through jointed rock mass is a complex phenomenon as the waves get transmitted and reflected at the joints. The seismic wave propagation results in the development of strains of varying levels, depending on the distance of the source of the vibration from the point of interest and the properties of the material through which it propagates. This paper describes the numerical simulation of a test facility that generates shear waves in rock plates. The numerical simulations have been developed with the help of a distinct element code program, three-dimensional distinct element code (3DEC). The test facility has an incident and transmitted plates along with a friction bar that produces shear waves in the incident plate, which are transmitted across the joint to reach the transmitted plate. The numerical simulation is validated by comparing the maximum particle velocities and maximum particle displacements developed in the incident and transmitted plates due to the propagation of waves, in the laboratory and in the numerical model. The wave energy that is transmitted and reflected at the rock joints has been calculated from the particle velocities obtained at the monitoring points. The ratio of the shear stresses due to the wave propagation at the monitoring points and the wave</p>

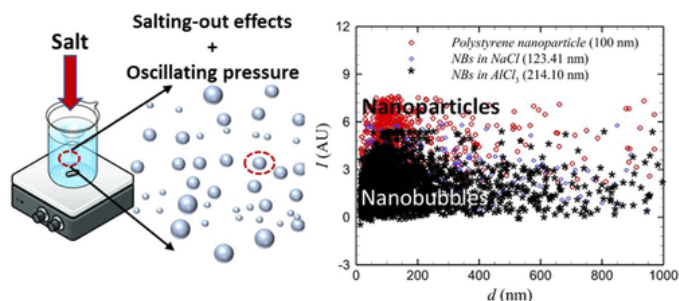
velocity reduction across the joint also have been calculated. A parametric study on the shear wave propagation has been conducted by varying the normal stress, properties of the joint and the magnitude of the load applied and the results are presented in this paper.

[On nanobubble dynamics under an oscillating pressure field during salting-out effects and its dlvo potential](#)

K Agarwal, M Trivedi, CD Ohl, N Nirmalkar - Langmuir, 2023

57.

Abstract: We have investigated the origin, stability, and nanobubble dynamics under an oscillating pressure field followed by the salting-out effects. The higher solubility ratio (salting-out parameter) of the dissolved gases and pure solvent nucleates nanobubbles during the salting-out effect, and the oscillating pressure field enhances the nanobubble density further as solubility varies linearly with gas pressure by Henry's law. A novel method for refractive index estimation is developed to differentiate nanobubbles and nanoparticles based on the scattering intensity of light. The electromagnetic wave equations have been numerically solved and compared with the Mie scattering theory. The scattering cross-section of the nanobubbles was estimated to be smaller than the nanoparticles. The DLVO potentials of the nanobubbles predict the stable colloidal system. The zeta potential of nanobubbles varied by generating nanobubbles in different salt solutions, and it is characterized by particle tracking, dynamic light scattering, and cryo-TEM. The size of nanobubbles in salt solutions was reported to be higher than that in pure water. The novel mechanical stability model is proposed by considering both ionic cloud and electrostatic pressure at the charged interface. The ionic cloud pressure is derived by electric flux balance, and it is found to be twice the electrostatic pressure. The mechanical stability model for a single nanobubble predicts the existence of stable nanobubbles in the stability map.



[On using non-Kekulé triangular graphene quantum dots for scavenging hazardous sulfur hexafluoride components](#)

V Roondhe, B Roondhe, S Saxena, R Ahuja, A Shukla - Heliyon, 2023

58.

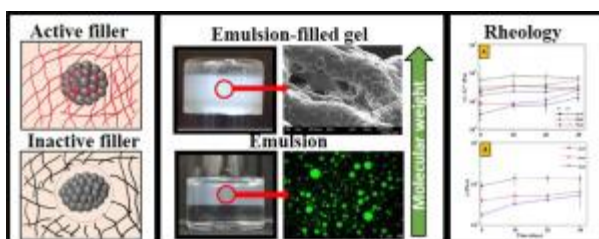
Abstract: The goal of present study is to explore how the size and functionalization of graphene quantum dots (GQDs) affect their sensing capabilities. Specifically, we investigated the adsorption of SO₂, SOF₂, SO₂F₂, and SF₆ on GQDs that were functionalized with -CH₃, -COCH₃, and -NH₂. We used density functional theory to analyse the electronic properties of these functionalized GQDs and found that the functionalization significantly altered their electronic properties. For example, the B3LYP H-L gap of pristine triangulene was 3.9eV, while the H-L gap of functionalized triangulene ranged from 2.8 eV to 3.6 eV (using the B3LYP functional). Our results indicate that -NH₂ functionalized phenalenyl and triangulene provide strong interaction with SO₂, with adsorption energies of -0.429 eV and -0.427 eV, respectively. These adsorption properties exhibit physisorption, leading to high gas sensitivity and superior recovery time. The findings of this study provide new insights into the potential use of GQDs for detecting the decomposed constituents of sulfur hexafluoride, which can be beneficial for assessing the operation status of SF₆ insulated devices. Overall, our calculations suggest that functionalized GQDs can be employed in gas insulated systems for partial discharge detection.

59.	<p>Optimal synthesis of reconfigurable manipulators for robotic assistance in vertical farming N Chitre, A Dogra, E Singla - Robotica, 2023</p> <p>Abstract: Due to the ever-increasing demand for food commodities and issues arising in their transport from rural to urban areas, commercial agricultural practices with the help of vertical farming are being taken up near urban regions. For the realization of agricultural practices on high-rise vertical farms, where human intervention is quite laborious, robotic assistance would be an effective solution to perform agricultural processes like seeding, transplanting, harvesting, health monitoring, nutrient-water supply, etc. The requirements and complexities of these tasks to be performed are different such as end-effector requirement, payload capacity required, amount of clutter while performing the task, etc. In such cases, an individual robotic configuration would not serve all the purposes and each task may require a different configuration. Purchasing a large number of configurations, as per requirement, is not economical and will also increase the cost of maintenance. Thus, the design of a reconfigurable robot manipulator is proposed in this work which can cater to modular layouts. A thorough study of the processes involved in the farming of leafy vegetables is done and the tasks to be performed by the manipulator are identified. Constrained optimization is performed based on reachability, while minimizing DoF, for the tasks of transplanting, plant health monitoring, and harvesting to find the optimal configurations which can perform the given tasks. The study resulted in 5-DoF, 4-DoF, and 6-DoF configurations for transplanting, plant health monitoring, and harvesting, respectively, thus emphasizing the need of a reconfigurable solution. The configurations are realized using modular library and verified to satisfy reachability to provide a complete solution.</p>
60.	<p>Performance analysis of solar rooftop systems based on racking arrangements in humid subtropical areas N Deka, MR Hazarika, S Bhardwaj - IEEE International Power and Renewable Energy Conference (IPRECON), 2023</p> <p>Abstract: Modern engineers find it often challenging to select an energy-efficient racking and the associated solar systems to harness maximum energy from the solar irradiance over a fixed rooftop area. Eight different solar rooftop systems are simulated in a software-based environment to find an optimal racking design associated with the solar design for a humid subtropical area within Guwahati city. Four different rackings (fixed-tilt, flush-mount, East-West and carport rackings) are arranged in horizontal and vertical orientations to measure the performance of these solar systems and identify the most efficient solar rooftop system in humid subtropical areas. Simulational analyses reveal that fixed-tilt, flush and carport systems arranged in vertical orientation can accommodate the maximum number of solar modules and frames and generate maximum AC and DC power of 48.1 kW and 59.2 kW. In-depth analyses of electrical parameters of the systems conclude that the vertically oriented carport system is the most efficient solar rooftop system suitable for humid subtropical areas of Guwahati city.</p>
61.	<p>Performance test of a position sensitive planar germanium detector for phase-III DESPEC A Sharma, R Palit, T Habermann...PP Singh - Nuclear Instruments and Methods in Physics Research Section A: Accelerators, Spectrometers, Detectors and Associated Equipment, 2023</p> <p>Abstract: The position sensitivity of a planar segmented double-sided germanium strip detector, with 10×10 electrical segmentation in orthogonal directions, has been studied using the coincidence method. The coincidences were set up between an imaging scanner and the PSPGe (Position Sensitive Planar Germanium) detector using a positron source, ^{22}Na, and analyzed by employing the Positron Annihilation Correlation principle. A collimated ^{241}Am source scan was also performed to find position resolution along X and Y axes using low energy gamma-ray source. The primary objective of this work is to study the charge carrier transportation for gamma-ray interactions inside the PSPGe detector. In order to select the electrodes of interest</p>

	<p>and to obtain the pulse shapes for each event, two-dimensional images have been processed. The net charge induced on the surface of the electrode, calculated using the pulse shape analysis procedure, has been used to profile the position resolution and gamma interaction depth. The present study is an input for the deployment of PSPGe detector in the future decay spectroscopy experiments to be performed at the Facility for Antiproton and Ion Research (FAIR) in Germany. This work investigates the gamma interaction depth by calculating the rise-time of traces stored for each gamma interaction inside the detector volume, providing ≈ 1 mm resolution along the depth. The position resolution of the detector in lateral directions, determined using the amplitude difference of the transient charges, has also been found to be ≈ 1 mm.</p>
62.	<p>Polymer composites for ion selective sensors M Kaur, N Kaur, N Singh - <i>Polymeric Nanocomposite Materials for Sensor Applications: A Book Chapter</i>, 2023</p> <p>Abstract: Important ionic species (metal ions and anions) play vital roles in environmental and biological systems; until recently, they have been detected by a variety of receptors based on organic dyes, inorganic quantum dots, carbon dots, organic nanoparticles, and many others that have been reported. Despite the progress made in this field, several problems and challenges still exist. Recently, polymer-based receptors have gained more attention from researchers because of their promising potential for biocompatibility, water-suspendability, photostability, fast radiative rate, large absorption coefficient, and excellent fluorescence properties. Hence, polymer nanocomposites (PNCs) cover a broad assortment of applications, including environmental remediation, nanoelectronics, nanocomposite-based drug delivery, bioimaging, etc. More importantly, the facile surface functionalization of PNCs has rendered them extremely suitable for the sensing of different analytes. This chapter provides a brief discussion of synthetic strategies for polymer-based nanocomposites, and then reviews PNC-based chemosensors for ionic species such as metal ions and anions.</p>
63.	<p>Preconcentration through self-assembled structure: Highly selective detection of aminoglycoside antibiotic in the contaminated water A Sharma, G Singh, S Saini, N Kaur, N Singh - <i>Sensors and Actuators B: Chemical</i>, 2023</p> <p>Abstract: The preconcentration of trace organic pollutants with low concentration in environmental water samples can be utilized as a significant approach to increase the sensitivity and accuracy of the particular detection system. Various nano-composite materials based on silver nanoparticles have proven potential for environment monitoring applications as they have cost-effectiveness and the highest quality factor in plasmonic ability in the spectrum from 300 to 1200 nm. In this context, herein, a short dipeptide was synthesized and thoroughly characterized by spectroscopic tools such as ^1H, ^{13}C NMR, FTIR, and ES-Mass spectrometry. Further, its organic nanoparticles (ONPs) were fabricated, and their nanocomposite with silver nanoparticles was prepared and validated by TEM, DLS, and UV-Visible spectroscopy. The developed ANS-H1 nanocomposite demonstrated selective colorimetric sensing of neomycin in water with a limit of detection of 70 pM. Further, the developed nanocomposite formed water-insoluble complexation with neomycin which constituted a rapid preconcentration step that may enhance sensing performance and brings the limit of detection (LOD) down to 23 pM. Thus, the present strategy for the selective detection of the trace organic pollutant neomycin possesses great potential for robust water quality for environment monitoring.</p>
64.	<p>Probing emulsion-gel transition in aqueous two-phase systems stabilized by charged nanoparticles: A simple pathway to fabricate water-in-water emulsion-filled gels C Shekhar, SG Marapureddy, V Mehandia...M Sabapathy - <i>Colloids and Surfaces A: Physicochemical and Engineering Aspects</i>, 2023</p> <p>Abstract: Nanoparticle-stabilized water-in-water (w/w) emulsions, an example of aqueous two-phase systems (ATPS), can produce low-fat food colloids, edible gels, bio-polymer-based bijels,</p>

scaffolds for tissue-engineering, and porous materials. This w/w emulsion is made from two thermodynamically incompatible aqueous-polymer solutions, such as polyethylene oxide (PEO) and dextran. Changing the molecular weight of PEO in one aqueous phase stabilises w/w emulsion. The state diagram we generated using electron and light microscopy provides a novel approach to producing stable emulsion-filled gels and emulsion droplets. The visual examination, brightfield, and fluorescent microscopy studies highlight the role of molecular weight and storage duration. The production of an emulsion-filled gel is ascribed to the “active-filler-particles” arrangement, typically seen when the affinity between droplets stabilised by particles and polymer is substantial. In contrast, we expect the “inactive-filler-particles” arrangement for the samples that undergo phase inversion. The temporal evolution of shear-induced structures recorded using a rheometer demonstrates that these emulsion-filled gels’ viscoelastic properties correspond directly with time, molecular weight, and polymer composition. The emulsion-filled gels generated displayed 90-day storage stability. Our work would help us understand the complex dynamics of w/w emulsion-based formulations that need suitable size, shape, appearance, and shelf life management.

Graphical abstract:



65.

[Quadra-stable dynamics of p53 and pten in the dna damage response](#)

S Gupta, PK Panda, DA Silveira, R Ahuja... - Cells, 2023

Abstract: Cell fate determination is a complex process that is frequently described as cells traveling on rugged pathways, beginning with DNA damage response (DDR). Tumor protein p53 (p53) and phosphatase and tensin homolog (PTEN) are two critical players in this process. Although both of these proteins are known to be key cell fate regulators, the exact mechanism by which they collaborate in the DDR remains unknown. Thus, we propose a dynamic Boolean network. Our model incorporates experimental data obtained from NSCLC cells and is the first of its kind. Our network’s wild-type system shows that DDR activates the G2/M checkpoint, and this triggers a cascade of events, involving p53 and PTEN, that ultimately lead to the four potential phenotypes: cell cycle arrest, senescence, autophagy, and apoptosis (quadra-stable dynamics). The network predictions correspond with the gain-and-loss of function investigations in the additional two cell lines (HeLa and MCF-7). Our findings imply that p53 and PTEN act as molecular switches that activate or deactivate specific pathways to govern cell fate decisions. Thus, our network facilitates the direct investigation of quadruplicate cell fate decisions in DDR. Therefore, we concluded that concurrently controlling PTEN and p53 dynamics may be a viable strategy for enhancing clinical outcomes.

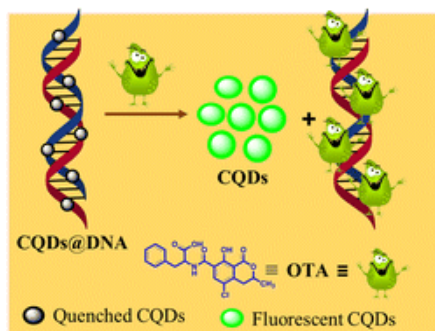
66.

[Quantitative and qualitative analysis of ochratoxin-A using fluorescent CQDs@DNA-based nanoarchitecture assembly to monitor food safety and quality](#)

A Singh, G Singh, N Kaur, N Singh - Analytical Methods, 2023

Abstract: Ochratoxin A (OTA), a mycotoxin formed by various fungi, such as *Aspergillus* and *Penicillium* species, is dangerous to human health. Thus, to circumvent the risk of OTA ingestion, the recognition and quantification of OTA levels are of great significance. A perusal of the literature has revealed that the integration of DNA/Carbon Quantum Dot

(CQD)-based hybrid systems may exhibit the unique electronic and optical properties of nanomaterials/nanoarchitecture and consequent recognition properties. Herein, we developed the CQDs@DNA-based hybrid nanoarchitecture system for the selective detection of OTA, which exhibits modulation in the emission spectrum after interaction with OTA, with a significant binding constant ($K_a = 3.5 \times 10^5 \text{ M}^{-1}$), a limit of detection of 14 nM, limit of quantification of 47 nM and working range of 1–10 μM . The mechanism for sensing the OTA has been corroborated using fluorescence, UV-visible absorption spectroscopy, and FTIR techniques, demonstrating the binding mode of CQD@DNA hybrid nano-architecture assembly with OTA. Further, we demonstrated the sensing ability of developed CQDs@DNA-based nanoarchitecture assembly towards the quantification of OTA in real food monitoring analysis for real-time applications, which makes this developed nanoarchitecture assembly the potential candidate to conveniently monitor food safety and quality for human health.



[Radial direction ultrasonic-vibration and laser assisted turning of Al3003 alloy](#)

N Deswal, R Kant - *Materials Research Express*, 2023

67.

Abstract: The utilization of various energy sources to assist the machining process has become prominent to obtain significant improvement in the machining performance. These energy sources have been utilized without using any cutting fluids which makes them eco-friendly. The combined action of laser and ultrasonic vibration energies during the turning process has shown significant achievement in machining process capabilities. Therefore, an attempt has been made to provide ultrasonic vibration in the radial direction and laser to preheat aluminium 3003 alloy simultaneously during the ultrasonic-vibration-laser assisted turning (UVLAT) process. Machining performance has been analyzed in terms of machining forces, machining temperature, chip morphology, surface damage, and surface roughness. A comparative machining performance analysis has been performed among the conventional turning (CT), ultrasonic vibration assisted turning (UVAT), laser assisted turning (LAT), and UVLAT processes. The outcomes of the present study revealed significant improvement in the machining performance for aluminium 3003 alloy during the UVLAT process. However, surface damage and surface roughness have been affected negatively during the UVLAT process due to the pin-point hammering and particle adhesion on the workpiece part. Hence, it can be said that the selection of vibration direction is a critical factor during the vibration machining processes.

[Real-time image based plant phenotyping using tiny-yolov4](#)

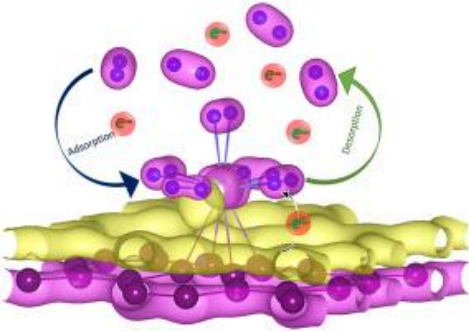
S Jain, D Mahapatra, M Saini - *International Conference on Intelligent Human Computer Interaction: Part of the Lecture Notes in Computer Science book series*, 2023

68.

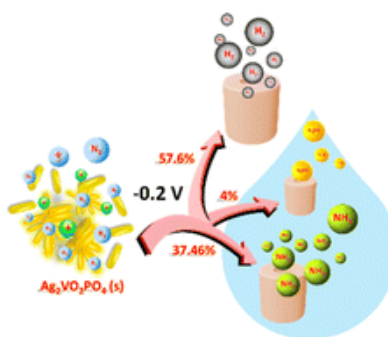
Abstract: Image-based plant phenotyping is getting considerable attention with the advancement in computer vision technologies. In the past few years, the use of deep neural networks (DNNs) is well-known for segmentation and detection tasks. However, most DNN-based methods require high computational resources, thus making them unsuitable for real-time decision-making. This study presents a real-time plant phenotyping system using leaf counting and tracking individual leaf growth. For leaf localization and counting, a Tiny-YOLOv4 network is utilized, which

	<p>provides faster processing, and is easily deployable on low-end hardware. Leaf growth tracking is performed by active contour segmentation of leaf localized using the Tiny-YOLOv4 network. The proposed system is implemented for top-view RGB images of the Arabidopsis thaliana' plants. And its performance for leaf counting is evaluated against Tiny-YOLOv3 and Faster R-CNN using the difference in count (DiC), accuracy, and F1-score measures. The model achieves an improved accuracy of 90%, absolute DiC of 0.42, F1-score of 96%, and inference time of 15 milliseconds. Further, the segmentation accuracy measures using Dice and Jaccard scores are 0.91 and 0.86, with a computing time of 0.96 s. These obtained results depict the effectiveness of the proposed system for real-time plant phenotyping.</p>
69.	<p>Reversible hydrogen storage tendency of light-metal (Li/Na/K) decorated carbon nitride (C₉N₄) monolayer SP Kaur, T Hussain, T Kaewmaraya, TJD Kumar - International Journal of Hydrogen Energy, 2023</p> <p>Abstract: The emergence of hydrogen (H₂) as a future carrier of energy and the issue related to its storage leads to the exploration of two-dimensional materials, which have the potential to be explored as H₂ storage materials. In this regard, potential of alkali metals (Li/Na/K) decorated two-dimensional carbon-nitride (C₉N₄) monolayer is studied for H₂ storage by performing first-principles density functional theory (DFT) computations. Metal dopants, Li, Na, and K show strong binding interactions with the C₉N₄ due to the transfer of charges from the formers to the later. In addition to strong bindings with C₉N₄ high diffusion barriers further nullify the cluster formation among metal dopants. The effect of temperature on the stability of alkali metal decorated C₉N₄ is studied in terms of ab-initio molecular dynamics (AIMD) simulations. The effect of metal decoration on electronic as well as magnetic properties of C₉N₄ are studied in terms of partial density of states (PDOS) plots. We find that each Li of Li-doped C₉N₄ (Li@C₉N₄) can stably binds six H₂ molecules without disintegration and results in the average adsorption energy of -0.20 eV, leading to a notably high H₂ storage capability of 11.9 wt%. Similarly, the storage capacities and average H₂ adsorption energies in the case of Na@C₉N₄ and K@C₉N₄ complexes fulfil the US Department of Energy (DOE) criteria. The electronic, AIMD, and thermodynamics analysis in this study provide an insight into that alkali metal decorated C₉N₄ as reversible H₂ storage material.</p>
70.	<p>Sheath voltage and sheath current phenomenon for different types of bonding for hv power cable under steady state A Das, CC Reddy - IEEE 6th International Conference on Condition Assessment Techniques in Electrical Systems (CATCON), 2023</p> <p>Abstract: Sheath being an eternal part of a cable, protects the insulation from moisture ingression, acts as an electrical shielding, and also a return path for load and fault current. Being grounded to at least any single point the cable sheath will always have either one of them or both types of phenomenon, the sheath voltage, and sheath current. The induced voltage in the sheath causes the flow of circulating current and this undesirable current causes sheath loss which affects the life expectancy of the cable. To reduce the sheath phenomenon different bonding system was introduced for the HVAC cable according to IEEE standard 575, but a single point, two points, and cross bonding cable are the most common phenomenon. In this paper, a comparative study of sheath voltage and sheath current for the different bonded systems is investigated, and a ladder network of the cable at a steady state was also mentioned. The simulation study was carried out with circuit-simulating software.</p>
71.	<p>Simulating radiofrequency ablation of hepatocellular carcinomas proximal to bare area of liver M Dhiman, R Repaka - Minimally Invasive Therapy & Allied Technologies, 2023</p> <p>Abstract: Purpose</p>

	<p>To numerically assess the significance of dextrose 5% in water (D5W) thermo-protection during radiofrequency ablation (RFA) of hepatocellular carcinomas (HCCs) located near the ‘bare area of liver’.</p> <p>Material and methods This study utilises quasi-anatomical structures extracted from CT images. A multi-tine electrode, deployed inside the extracted organs and operated under temperature-controlled mode was used as the source of ablation. Geometrically, D5W was modelled around the ‘bare area’ and sandwiched between the liver and diaphragm. RFA at different sites relative to the ‘bare area’ was simulated to answer when to consider modelling D5W.</p> <p>Results For targets near the edge of ‘bare area’ and at 0.5 mm gap (between the electrode and the ‘bare area’), ignoring D5W and using ground conditions could result in underestimation of ablation volume by almost 25%. The importance of D5W becomes negligible for ablations near the centre of the ‘bare area’.</p> <p>Conclusions Consideration of D5W during RFA of HCCs proximal to the ‘bare area’ can significantly influence the ablation outcome, especially when ablation is performed near the edge of the ‘bare area’.</p>
72.	<p>Single target visual object tracking S Kumar, SK Singh - Advanced Computing and Communication Technologies for High Performance Applications (ACCTHPA): A Conference Proceeding, 2023</p> <p>Abstract: In the present world, the evolution of technology takes place in terms of developing new things to solve some real-world problems. Almost all fields are creative in the sense of creating new things. Computer vision is one of the fields that give the technology that can help with different real-time problems. This field offers some useful applications over the last few decades. Different technologies like Autonomous cars, Traffic flow analysis, X-ray analysis, etc. make this field interesting for researchers. Object detection is one of the applications of Computer vision. Object detection and tracking enable the machine to detect the object and track the object through the entire scene. In this paper, a supervised learning approach for object detection is presented which consists of a detector, a Neural network, Images, and Groundtruths. The presented model successfully tracks the object and the dataset used for the performance evaluation is Online Object Tracking Benchmark (OOTB), Unmanned Aerial Vehicle (UAV), and Visual Object Tracking Benchmark (VOT) dataset.</p>
73.	<p>Social network analysis of the caste-based reservation system in india A Saxena, N Sethiya, JS Saini, Y Gupta, SRS Iyengar - Computational Data and Social Networks: Part of the Lecture Notes in Computer Science book series, 2023</p> <p>Abstract: Being as old as human civilization, discrimination based on various grounds such as race, creed, gender, and caste has existed for a long time. To undo the impact of this long-enduring historical discrimination, governments worldwide have adopted various forms of affirmative action, such as positive discrimination, employment equity, and quota system. In India, people are considered to belong to Backward Class (BC) or Forward Class (FC), and the Indian government designed an affirmative action, locally known as the “Reservation” policy, to reduce the discrimination between both groups. Through this affirmative action, the government provides support to people from the backward class (BC). Although being one of the most controversial and frequently debated issues, the reservation system in India lacks rigorous scientific study and analysis. In this paper, we model the dynamics of the reservation system based on the cultural divide among the Indian population using social network analysis. The mathematical model, using the Erdős-Rényi network, shows that the addition of weak ties between the two groups leads to a logarithmic reduction in the social distance. Our experimental simulations establish the claim for the different clans of frequently studied social network</p>

	<p>models as well as real-world networks. We further show that a small number of links created by the reservation process are adequate for a society to live in harmony.</p>
74.	<p>Studies on structural changes of modified mwcnts: material for electrochemical monitoring of antiviral drug in human serum samples R Kaur, G Bhardwaj, N Singh, N Kaur – Chemistry A European Journal, 2023</p> <p>Abstract: The development of a universal approach for precisely tuning the electrochemical characteristics of conducting carbon nanotubes for tracking harmful agents in the human body with high selectivity and sensitivity remains a challenge. Herein, we describe a simplistic, versatile, and general approach to the construction of functionalized electrochemical material. The design of electrochemical material consists of (i) modification of multiwalled carbon nanotubes (MWCNT) with dipodal naphthyl-based dipodal urea (KR-1) through non-covalent functionalization (KR-1@MWCNT) which enhances the dispersibility of MWCNT and hence conductivity, (ii) complexation of KR-1@MWCNT with Hg^{2+} accelerate the electron transfer in the material which amplify the detection response of functionalized material (i. e., Hg/KR-1@MWCNT) towards various thymidine analogues. Further, the application of functionalized electrochemical material (Hg/KR-1@MWCNT) achieves real-time electrochemical monitoring of harmful antiviral drug 5-iodo-2'-iododeoxyuridine (IUdR) levels in human serum for the first time.</p>
75.	<p>Superior hydrogen storage capacity of Vanadium decorated biphenylene (Bi+V): A DFT study P Mane, SP Kaur, M Singh, A Kundu... - International Journal of Hydrogen Energy, 2023</p> <p>Abstract: Herein, the hydrogen storage competency of vanadium-decorated biphenylene (Bi+V) has been investigated using Density Functional Theory simulations. The metal atom interacts with biphenylene with a binding energy value of -2.49 eV because of charge transfer between V 3d and C 2p orbitals. The structure and electronic properties are studied in terms of adsorption energy values, the spin-polarized partial density of states (PDOS), band structure plots, and charge transfer analysis. The Kubas-type interactions lead to average hydrogen adsorption energy values of -0.51 eV/H_2 which fulfills DOE-US criteria (0.2–0.7 eV/H_2). The diffusion energy barrier value of 1.75 eV lowers the chances of metal clustering. The complex binds 5H_2 on each V-atom resulting in a storage capacity of 7.52 wt% with an average desorption temperature of 595.96 K. The ab-initio molecular dynamics (AIMD) and phonon dispersions validates structural integrity at higher temperatures suggesting the excellent storage properties of this material at room temperature.</p> <p>Graphical abstract:</p> 
76.	<p>Sustainable ammonia synthesis through electrochemical dinitrogen activation using an $\text{Ag}_2\text{VO}_2\text{PO}_4$ catalyst D Gupta, A Kafle, TC Nagaiah - Faraday Discussions, 2023</p> <p>Abstract: Ammonia (NH_3) is the second most produced chemical commodity with a worldwide</p>

production of 235 million tonnes in 2019, by virtue of its importance in fertilizer production, energy storage and transportation, and in the production of industrial chemicals. The most frequent method of NH_3 production in large plants (1000 to 1500 t day^{-1}) is the Haber–Bosch process, which has drawbacks of high greenhouse gas emissions (2.16 tonnes CO_2 per tonne of NH_3) and high energy consumption (over 30 GJ per tonne of NH_3) due to high pressure and temperature conditions. For sustainable NH_3 production, we require alternative green routes, wherein the electrochemical route holds huge potential due to reduced energy consumption and plant costs, higher selectivity, lower temperatures and pressures, and small to medium scale utilization of NH_3 . However, there are a number of challenges faced during the same *viz.* low production rates due to difficult N_2 activation and reduced faradaic efficiency due to competing side reactions in aqueous electrolytes. Therefore, the most crucial aspect of electrochemical ammonia production technology is the design of an electrocatalyst which could activate the strong $\text{N}\equiv\text{N}$ triple bond and effectively suppress the competing hydrogen evolution reaction (HER). In addition, the true NH_3 yield estimation is of major concern due to the presence of possible N-contaminants, which may possibly lead to false estimation or overestimation of NH_3 . In this context, we have synthesized an $\text{Ag}_2\text{VO}_2\text{PO}_4$ electrocatalyst with rice-grain like morphology *via* an energy efficient and less time consuming sonochemical method to carry out low temperature NH_3 synthesis in an alkaline electrolyte. The choice of Ag metal and an alkaline environment effectually suppresses the HER and the bimetallic phosphate materials (Ag and V metals) induce high activity during nitrogen reduction, while rigorous analysis for tracing/elimination of N-labile and reducible species is considered for true NH_3 production and assessment.



[The expectation-maximization algorithm for autoregressive models with normal inverse Gaussian innovations](#)

MS Dhull, A Kumar... - Communications in Statistics - Simulation and Computation, 2023

77.

Abstract: In this paper, we study the autoregressive (AR) model with normal inverse Gaussian (NIG) innovations. The NIG distribution is semi heavy-tailed and is helpful in capturing the extreme observations present in the data. The expectation-maximization (EM) algorithm is used to estimate the parameters of the considered $\text{AR}(p)$ model. The efficacy of the estimation procedure is shown on the simulated data for $\text{AR}(2)$ and $\text{AR}(1)$ models. A comparative study is presented, where the classical estimation algorithms are also incorporated, namely, Yule-Walker and conditional least squares methods along with EM method for model parameter estimation. In simulation study, the maximum likelihood estimation (MLE) of NIG distribution by EM algorithm and iterative Newton-Raphson method are also compared. The real-life applications of the introduced model are demonstrated on the NASDAQ stock market index data and US gasoline price data. The studies show that $\text{AR}(1)$ model with NIG residuals is good fit for financial data with extreme values as well as for gasoline price data.

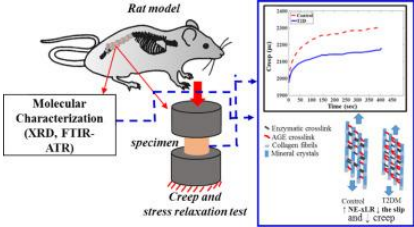
78.

[Thermal runaway state in lithium ion batteries of electric vehicles: an overview](#)

A Ahmad, AVR Teja, S Payami - IEEE International Conference on Power Electronics, Drives and Energy Systems (PEDES), 2023

	<p>Abstract: Lithium Batteries possess the highest marketplace in the energy storage industry despite the fact that safety is always an open challenge for the designers, especially for EVs, which include the thermal runaways (TR). This manuscript provides sufficient information in order to make the reader understand the basics of thermal runaway, the chemical alteration due to electrical effect that forms dendrite on electrodes and the apparent causes that led to the TR in the first place. Sufficient research is done enough to understand the process and to analyse the same. The effects of electrical and mechanical abuse on the battery are explained. Several methods to detect the TR has been discussed which can be addressed as a scope to further the research for online detection of TR</p>
79.	<p>Thermal stability and decomposition mechanisms of hexatetracarbon: Tight-binding molecular dynamics and density functional theory study Y Bauetdinov...R Sangwan - <i>Modern Physics Letters B</i>, 2023</p> <p>Abstract: In this work, we carry out molecular dynamics and <i>ab initio</i> modeling to determine the thermal decomposition channels and thermal stability of the recently proposed 2D carbon allotrope, hexatetracarbon (HTC). To take into account the role of edges in the initialization of decay, we considered finite size cluster models of HTC passivated by hydrogen. Four models were selected for the study: $C_{12}H_{12}$, $C_{12}H_{12}$, $C_{20}H_{16}$, $C_{20}H_{16}$, $C_{26}H_{18}$, $C_{26}H_{18}$ and $C_{48}H_{24}$, $C_{48}H_{24}$. Molecular dynamics and hyperdynamics was carried out using the NTBM non-orthogonal tight-binding model. For <i>ab initio</i> calculations, we used the electron density functional theory with the B3LYP three-parameter hybrid functional and the 6-311G*** electronic basis set. Prismane $C_{12}H_{12}$ demonstrated the highest stability due to the high energy barrier of 1.5 eV preserving its decomposition. Larger clusters possessed lower barriers in the 0.65–0.9 eV range. We concluded that the HTC edges are unstable at room temperatures. However, the destruction of some interlayer bonds can result in strain relaxation and increase of stability. We believe that HTC could exist at room temperatures in the form of nanosized quantum dots that appeared from bilayer graphene under high pressure.</p>
80.	<p>Toroidal-ee-based integrated common-mode choke for dc-side emi filter S Singh, B Dwiza, NB Gorla, J Kalaiselvi - <i>IEEE IAS Global Conference on Renewable Energy and Hydrogen Technologies (GlobConHT)</i>, 2023</p> <p>Abstract: In literature, the use of passive electromagnetic interference (EMI) filters is extensively researched to not only restrain the common-mode (CM) noise but also the differential-mode (DM) noise. Although the CM and DM chokes are simple to design, reliable, and do not need an auxiliary power supply, they increase the overall volume and reduce the power density of a power converter. Hence, this paper presents a novel integrated choke that offers higher DM impedance than the traditional CM choke by maintaining the same volume, when compared to the traditional CM choke. The calculation of CM inductance, as well as DM inductance of the proposed integrated filter topology, is presented along with a small signal measurement using an impedance analyzer. The proposed EMI filter performance is verified on a three-phase silicon carbide (SiC) fed brushless dc (BLdc) motor.</p>
81.	<p>Towards accessible chart visualizations for the non-visually impaired: Research, applications and gaps M Singh, MS Kanroo, HS Kawoosa, P Goyal - <i>Computer Science Review</i>, 2023</p> <p>Abstract: Chart Visualizations (<i>CharVis</i>) such as charts/plots and diagrams are commonly used in documents for representing the underlying quantitative information. However, the inaccessibility of such visualizations exemplify one of the rife challenges of information access for Blind and Visually Impaired People (BVIP). The existing BVIP-related assistive technologies (ATs) are capable enough to provide the accessibility of textual components; however, for <i>CharVis</i>, it is of concern. Unlike textual components, <i>CharVis</i> comprise critical compressed data and requires perspicacious reverse-engineering schemes to output the raw data</p>

	<p>table used initially for creation. An intelligent and automated BVIP-compatible <i>CharVis</i> understanding scheme requires extraction of raw underlying data and presenting it into BVIP-compatible representation, i.e., summarized audio form. With the recent advancements in rapidly-growing AI-domain, several frameworks have been proposed in the literature for accurate extraction of the raw content from <i>CharVis</i>. Most of the existing related work and surveys emphasize only the visualization-related aspects without considering the apprehensions regarding inclusivity of these visualization schemes for BVIP. This survey aims to analyze various research methodologies on the <i>CharVis</i> understanding process, and related existing and potential assistive applications in a threefold outcome manner - (1) Research: We provide a perspicuous investigation of state-of-the-art research methodologies for <i>CharVis</i> understanding. (2) Applications: We provide a detailed rubric analysis of various applications and compatible assistive solutions (3) Gap: We summarize the challenges and the gaps between the research and application domain and provides new insights/pointers for future research. Additionally, the survey presents a consolidated list of datasets, software/apps, and hardware sources for supporting future research.</p>
82.	<p>Transformer equivalent model of sheathed cable M Khadka, P Johri, CC Reddy - IEEE 6th International Conference on Condition Assessment Techniques in Electrical Systems (CATCON), 2023</p> <p>Abstract: The metallic sheath in cables is supposed to carry a substantial current mainly during ground faults and also acts as a return path for capacitive charging current. However, electromagnetic coupling between the conductor and the metallic sheath may lead to induction of emf. The induced emf is responsible for an additional current in the sheath, which may pose certain problems. The existing methods of sheath current calculations tend to involve mathematical complexities and thus a simplified circuit model is desirable. This paper focuses on finding resemblance of metallic sheathed cable with transformer and proposes an equivalent circuit model. Experimental methods are presented to estimate the series parameters of the equivalent model and also to estimate the effective transformation ratio. The results are validated through comparison with simulation and approximate analytical results and were found to be in agreement.</p>
83.	<p>Type 2 diabetes alters the viscoelastic behavior and macromolecular composition of vertebra D Mehta, P Sihota, K Tikoo, S Kumar, N Kumar - Bone Reports, 2023</p> <p>Abstract: Type 2 diabetes (T2D) affects the functional behavior of vertebra bone by altering its structural and mechanical properties. The vertebral bones are responsible to carry the body weight and it remains under prolonged constant load which results to viscoelastic deformation. The effect of T2D on the viscoelastic behavior of vertebral bone is not well explored yet. In this study, the effects of T2D on the creep and stress relaxation behavior of vertebral bone are investigated. Also, this study established a correlation between T2D associated alteration in macromolecular structure and viscoelastic behavior of vertebra. In this study T2D female rat SD model was used. The obtained results demonstrated a significant reduction in the amount of creep strain ($p \leq 0.05$) and stress relaxation ($p \leq 0.01$) in T2D specimens than the control. Also, the creep rate was found significantly lower in T2D specimens. On the other hand, molecular structural parameters such as mineral-to-matrix ratio (control vs T2D: 2.93 ± 0.78 vs 3.72 ± 0.53; $p = 0.02$), and non-enzymatic cross link ratio (NE-xL) (control vs T2D: 1.53 ± 0.07 vs 3.84 ± 0.20; $p = 0.01$) were found significantly altered in T2D specimens. Pearson linear correlation tests show a significant correlation; between creep rate and NE-xL ($r = -0.94$, $p < 0.01$), and between stress relaxation and NE-xL ($r = -0.946$, $p < 0.01$). Overall this study explored the understanding about the disease associated alteration in viscoelastic response of vertebra and its correlation with macromolecular composition which can help to understand the disease related impaired functioning of the vertebrae body.</p>

	<p>Graphical abstract: An investigation on the effects of T2DM on the viscoelastic and macromolecular properties of vertebral body in female SD rat.</p> 
84.	<p>Understanding stable/unstable miscible $A+B \rightarrow C$ reaction front and mixing in porous medium P Verma, V Sharma, M Mishra - Physics of Fluids, 2023</p> <p>Abstract: The transport phenomena of $A + B \rightarrow C$ type reactive miscible front undergoing radial displacement in a porous medium are numerically investigated. For a stable displacement when the viscosity of fluids A, B, and C is same, the dependence of various reaction characteristics on the Damköhler number (Da) is analyzed. The total reaction rate is found to be a non-monotonic function of time depending upon Da, while the total amount of product follows the temporal scaling $\propto t f(Da)$. The viscosity contrast in the system renders unstable flow and results in a hydrodynamic instability called viscous fingering. The effect of hydrodynamics on the reaction product formation is discussed. An insight into the reaction characteristics due to interaction of chemical reaction and instability is obtained for various log-mobility ratios R_b and R_c. It is observed that the onset of instability, as well as the mixing of the fluids, depends on whether the reaction generates a high or less viscous product or equivalently, the sign of $R_b - R_c$, keeping R_b fixed. Furthermore, the relation between the first moment of averaged reaction rate for stable and unstable displacement is influenced by the sign of $R_b - R_c$ and Da. The coupling of convection and diffusion on the chemo-hydrodynamic instability is presented, and the existence of the frozen fingers in this reactive fluid system is reported. Our numerical results allow us to understand how instability and chemical reaction interplay to affect the reaction characteristics and the mixing of fluids.</p>
85.	<p>Understanding the low-energy incomplete fusion reactions A Yadav, G Ram, MS Asnain, I Majeed, M Shuaib...PP Singh... - Physical Review C, 2023</p> <p>Abstract: With a motivation to find out the systematics for the low-energy ($\approx 4-7$ MeV/nucleon) incomplete fusion reactions, the experimentally measured excitation functions for evaporation residues, which were populated during the interactions of ^{18}O with ^{159}Tb target nuclei, have been studied. The analysis clearly exhibits that the xn/pxn channels are populated to a large extent through the complete fusion processes. Although, the production cross-section of the α-emitting channels, despite of deducting the precursor decay contribution, found to be significantly underestimated by the statistical model predictions. The observed enhancement, which may be attributed due to the involvement of break-up fusion processes, is found to be get larger with the incident energy. In addition, the present work in light of the literature data imparts the reliance of incomplete fusion processes on various entrance channel parameters, such as the mass-asymmetry of the interacting partners, fissility parameter and also on the $Z_p Z_T$ (Coulomb factor). These systematics inarguably indicates the projectile type dependency of the incomplete fusion reactions, and the results may be explained on the basis of the $\alpha-Q$ value of the projectile. Furthermore, an attempt has been made to explain the trends of incomplete fusion fractions through the total asymmetry parameter and the system parameter, where system parameter seems to explain the data more satisfactorily, as it incorporates the Coulomb factor as well as the masses of the interacting partners.</p>
86.	<p>Voltage support and imbalance mitigation during voltage sags by renewable energy fed grid</p>

[connected inverters](#)

AH Lone, AI Gedam, KR Sekhar - IEEE IAS Global Conference on Renewable Energy and Hydrogen Technologies (GlobConHT), 2023

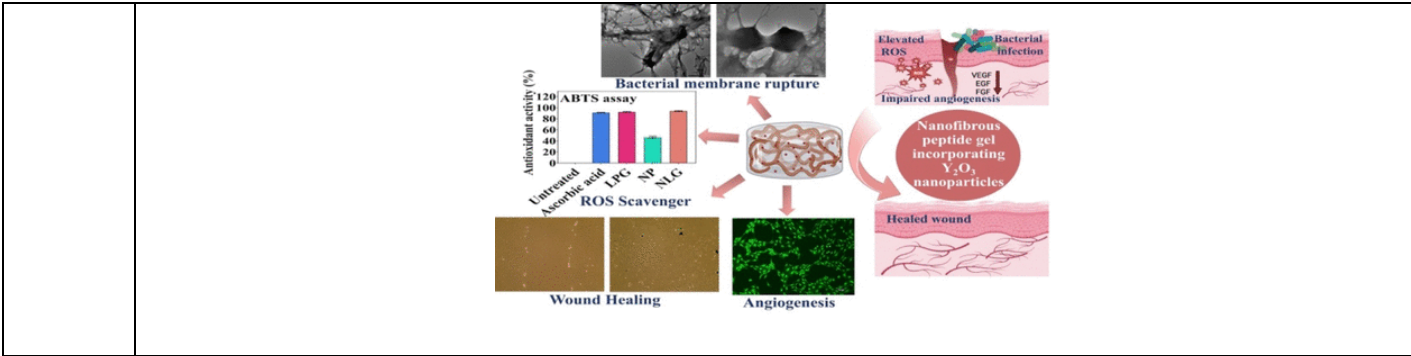
Abstract: In this study, symmetrical component-based current injection is used to analyse a single-stage grid-connected inverter with low voltage ride-through (LVRT) capability. During voltage sags, the renewable source-fed voltage source inverter (VSI) may disconnect from the main grid at the point of common coupling. This condition arises due to the Under-voltage/over-current protection in the renewable inverters. This sudden dis-connecting of the inverters may cause voltage collapse, frequency instability, and synchronous angle instability in utility networks with significant penetration of power from renewable inverters, which can result in blackouts. Utility grid rules require low-voltage ride-through capabilities in grid-connected inverters to mitigate this effect. In order to support voltage and reduce volt-age imbalance at the point of common coupling, a symmetrical component-based real and reactive power injection approach has been developed in this study. This technique is implemented by considering the constraint of not exceeding the inverter's rated current capability. The proposed technique effectively boosted the positive sequence voltage component to a reference value by using a PI controller. The negative sequence reactive power was drawn using the remaining reactive power capacity in order to suppress the voltage's negative sequence component. Results are presented in the paper for various voltage sag conditions. The proposed techniques are validated by simulating the model in a Matlab simulink environment.

[Yttrium oxide nanoparticle-loaded, self-assembled peptide gel with antibacterial, anti-inflammatory, and proangiogenic properties for wound healing](#)

V Chawla, S Sharma, Y Singh - ACS Biomaterials Science & Engineering, 2023

87.

Abstract: Chronic wounds are a major healthcare challenge owing to their complex healing mechanism and number of impediments to the healing process, like infections, unregulated inflammation, impaired cellular functions, poor angiogenesis, and enhanced protease activity. Current topical care strategies, such as surgical debridement, absorption of exudates, drug-loaded hydrogels for infection and inflammation management, and exogenous supply of growth factors for angiogenesis and cell proliferation, slow the progression of wounds and reduce patient suffering but suffer from low overall cure rates. Therefore, we have developed a proteolytically stable, multifunctional nanoparticle loaded-peptide gel with inherent anti-inflammatory, antibacterial, and pro-angiogenic properties to provide a favorable wound healing milieu by restoring impaired cellular functions. We have fabricated a self-assembled, lauric acid-peptide conjugate gel, LA-^LLys-^DPhe-^LLys-NH₂, loaded with yttrium oxide (Y₂O₃) nanoparticles (NLG). Gel formed a nanofibrous structure, and nanoparticles were passively entrapped within the network. The surface morphology, stability, viscoelastic, and self-healing characteristics of gels were characterized. It showed a high stability against degradation by proteolytic enzymes and highly potent antibacterial activities against *E. coli* and *S. aureus* due to the presence of positively charged side chains of lysine in the peptide chain. It also exhibited an excellent antioxidant activity as well as ability to stimulate cell proliferation in murine fibroblast (L929) cells and human umbilical vein endothelial cells (HUVECs). The incorporation of nanoparticles promoted angiogenesis by upregulating pro-angiogenic genes, vascular endothelial growth factor (VEGF), fibroblast growth factor (FGF2), and epidermal growth factor (EGFR), and the gel caused complete wound closure in cells. In summary, the Y₂O₃ nanoparticle-loaded lauric acid-peptide conjugate gel is able to elicit the desired tissue regeneration responses and, therefore, has a strong potential as a matrix for the treatment of chronic wounds.



Disclaimer: This publication digest may not contain all the papers published. Library has compiled the publication data as per the alerts received from Scopus and Google Scholar for the affiliation “Indian Institute of Technology Ropar” for the month of April 2023. The author(s) are requested to share their missing paper(s) details if any, for the inclusion in the next publication digest.